JPET Fast Forward. Published on April 7, 2017 as DOI: 10.1124/jpet.116.239707
This article has not been copyedited and formatted. The final version may differ from this version.

Regulation of UGT2B4 and UGT2B7 by miRNAs in liver cancer cells

Dhilushi D Wijayakumara, Peter I Mackenzie, Ross A McKinnon, Dong Gui Hu* and Robyn Meech*

Department of Clinical Pharmacology and Flinders Centre for Innovation In Cancer, Flinders University School of Medicine, Flinders Medical Centre, Bedford Park SA 5042, Australia
* Co-last authors

Downloaded from jpet.aspetjournals.org at ASPET Journals on March 20, 2024

JPET Fast Forward. Published on April 7, 2017 as DOI: 10.1124/jpet.116.239707
This article has not been copyedited and formatted. The final version may differ from this version.

Running title: Regulation of UGT2B4 and UGT2B7 by miRNA

Address correspondence to

Dr Robyn Meech

Department of Clinical Pharmacology, Flinders University School of Medicine, Flinders Medical Centre, Bedford Park SA 5042, Australia

Phone: 61 8 82044795

Fax: 61 8 82045114

Email: robyn.meech@flinders.edu.au

Number of text pages: 18

Number of Tables: 1

Number of Figures: 5

Number of References: 60

Number of words in Abstract: 252

Number of words in Introduction: 598

Number of words in Discussion: 1365

Downloaded from jpet.aspetjournals.org at ASPET Journals on March 20, 2024

JPET Fast Forward. Published on April 7, 2017 as DOI: 10.1124/jpet.116.239707
This article has not been copyedited and formatted. The final version may differ from this version.

Abbreviations:

miR:	microRNA
miRNA:	microRNA
miR-neg:	negative control microRNA
PCR:	polymerase chain reaction
RNA-seq:	RNA- sequencing
RNU6-2:	U6 small nuclear-2 RNA
RT-qPCR:	quantitative real-time polymerase chain reaction
UGT:	UDP-glucuronosyltransferase
UTR:	untranslated region
miRISC:	miRNA-induced silencing complex
TCGA:	The Cancer Genome Atlas
TCGA-LIHC:	The Cancer Genome Atlas Liver Hepatocellular Carcinoma collection
UGT:	UDP-glucoronosyltransferase

Downloaded from jpet.aspetjournals.org at ASPET Journals on March 20, 2024

JPET Fast Forward. Published on April 7, 2017 as DOI: 10.1124/jpet.116.239707
This article has not been copyedited and formatted. The final version may differ from this version.

Abstract

The transcriptional regulation of *UGT2B4* and *UGT2B7* has been well studied using liver cancer cell lines and recently post-transcriptional regulation of these two *UGTs* by miR-216b-5p was reported. The present study describes novel miRNA-mediated regulation of UGT2B4 and UGT2B7 in liver cancer cells. Bioinformatic analyses identified a putative miR-3664-3p binding site in the UGT2B7 3'-UTR, and binding sites for both miR-135a-5p and miR-410-3p in the UGT2B4 3'-UTR. These sites were functionally characterized using miRNA mimics and reporter constructs. A miR-3664-3p mimic induced repression of a luciferase reporter carrying the UGT2B7 3'-UTR in liver cancer cell lines; mutation of the miR-3664-3p site abrogated the response of the reporter to the mimic. Similarly, mutation of the miR-135a-5p site or miR-410-3p site in a luciferase reporter bearing UGT2B4 3'-UTR abrogated the ability of miR-135a-5p or miR-410-3p mimics to reduce reporter activity. Transfection of miR-3664-3p mimics in HepG2 liver cancer cells significantly reduced mRNA and protein levels of UGT2B7, and this led to reduced enzymatic activity. Transfection of miR-135a-5p or miR-410-3p mimics significantly decreased UGT2B4 mRNA levels in Huh7 liver cancer cells. The expression levels of miR-410-3p were inversely correlated with UGT2B4 mRNA levels in the TCGA cohort of Liver Hepatocellular Carcinoma (371 specimens) and a panel of 9 normal human tissues. Similarly, there was an inverse correlation between miR-135a and UGT2B4 mRNA levels in a panel of 18 normal human liver tissues. Together these data suggest that miR-135a and miR-410 control *UGT2B4* and that miR-3664 controls *UGT2B7* expression in liver cancer and/or normal liver cells.

Downloaded from jpet.aspetjournals.org at ASPET Journals on March 20, 2024

JPET Fast Forward. Published on April 7, 2017 as DOI: 10.1124/jpet.116.239707
This article has not been copyedited and formatted. The final version may differ from this version.

Introduction

Glucuronidation refers to the covalent attachment of glucuronic acid to a variety of endogenous and exogenous small lipophilic compounds; glucuronidated products are generally biologically inactive and more water soluble, thus facilitating their excretion from the body (Mackenzie et al., 2005, Mackenzie et al., 1997). There are four human UDP glucuronosyltransferase (UGT) families (Mackenzie et al., 2005); however, glucuronidation is primarily carried out by members of the UGT1A and UGT2B subfamilies. Substrates for these enzymes include endogenous bioactive molecules (e.g. steroids, thyroid hormones, bilirubin, bile acids, retinoids, fatty acids), carcinogens, environmental pollutants, and therapeutic drugs (Mackenzie et al., 2005, Guillemette, 2003). It was estimated that UGTs are involved in the metabolism of 35% of clinically administered drugs (Guillemette, 2003).

The liver is the primary site of glucuronidation and thus the control of hepatic UGT expression and activity is of significant biological and pharmacological interest (Hu et al., 2014b). UGT2B4 and UGT2B7 are both highly expressed in the liver (Congiu et al., 2002, Court, 2010). UGT2B7 has high activity towards various endogenous compounds including bile acids, retinoic acids, steroids, mineralocorticoid and glucocorticoid hormones and fatty acids (Hu et al., 2014b) as well as exogenous compounds including carcinogens, therapeutic drugs such as morphine, codeine (Coffman et al., 1997), epirubicin (Innocenti et al., 2001), valproic acid (Argikar and Remmel, 2009), and nonsteroidal anti-inflammatory drugs (Jin et al., 1993). Around 35% of the therapeutic drugs that are glucuronidated by UGTs are UGT2B7 substrates (Williams et al., 2004). In addition to hepatic expression, UGT2B7 is expressed in small intestine, colon, kidney, and breast where it may also play important roles in drug metabolism and homeostasis of endogenous bioactive molecules (Ohno and Nakajin,

Downloaded from jpet.aspetjournals.org at ASPET Journals on March 20, 2024

JPET Fast Forward. Published on April 7, 2017 as DOI: 10.1124/jpet.116.239707
This article has not been copyedited and formatted. The final version may differ from this version.

2009, Hu et al., 2014b). UGT2B4 is also abundantly expressed in many extrahepatic tissues and organs (e.g. kidney and esophagus) (Ohno and Nakajin, 2009) and has an important role in the glucuronidation of bile acids (Fournel-Gigleux et al., 1989), catechol-estrogens (Ritter et al., 1992), androgen metabolites (Lepine et al., 2004, Levesque et al., 1999, Turgeon et al., 2001),,and phenols (Guillemette, 2003). UGT2B4 is involved in the glucuronidation of hydroxylated bile acids (Barre et al., 2007); as well as a subset of drugs and toxins including deoxynivalenol (a mycotoxin) (Maul et al., 2014), hydroxymidazolam (Seo et al., 2010), lorazepam (Uchaipichat et al., 2013), codeine (Raungrut et al., 2010), eslicarbazepine (an antiepileptic) (Loureiro et al., 2011), and carvedilol (a β-adrenoceptor blocker) (Ohno et al., 2004). However in general UGT2B4 is considered to play a more minor role in overall drug metabolism than UGT2B7.

As recently reviewed (Hu et al., 2014b), the transcriptional regulation of *UGT2B4* and *UGT2B7* has been well investigated using hepatic models such as liver cancer cell lines, human primary hepatocytes, and transgenic mice. The transcription factors that have been found to be involved in controlling UGT2B7 expression include hepatocyte nuclear factor 1α (HNF1α) (Ishii et al., 2000), HNF4α, caudal related homeobox factor 2 (Cdx2) (Gregory et al., 2006), Nuclear factor (erythroid-derived 2)-like 2 (Nrf2) (Nakamura et al., 2008), Farnesoid X receptor (FXR) (Lu et al., 2005), p53 (Hu et al., 2014c), and activator protein 1 (AP-1) proteins (Hu et al., 2014a). UGT2B4 is known to be transcriptionally regulated by FXR, retinoid X receptor (RXR), and peroxisome proliferator activated receptor α (PPARα) (Barbier et al., 2003a, Barbier et al., 2003b). MicroRNAs (miRNAs) are non-coding small RNAs (~21-25 nt) that mediate post-transcriptional gene regulation through translational repression and/or mRNA degradation (Macfarlane and Murphy, 2010). The first identification of a miRNA involved in *UGT2B4* and *UGT2B7* regulation (miR-216b-5p) in liver cancer cell lines was recently reported (Dluzen et al., 2016). The present study provides

Downloaded from jpet.aspetjournals.org at ASPET Journals on March 20, 2024

JPET Fast Forward. Published on April 7, 2017 as DOI: 10.1124/jpet.116.239707
This article has not been copyedited and formatted. The final version may differ from this version.

in depth characterization of the roles of three additional miRNAs, miR-3664-3p, miR-135a-5p and miR-410-3p, in regulation of *UGT2B4* and *UGT2B7* in liver cancer cell lines.

Materials and Methods

miRNA Mimics and Human Tissue Total RNA. Mimics of hsa-miR3664-3p, hsa-miR-135a-5p, hsa-miR-410-3p, hsa-miR-1266-5p, hsa-miR-4483, hsa-miR-4317, hsa-miR216b-5p,has-miR-489-3p, hsa-miR-4691-5p, hsa-miR-101-3p, and a negative control miRNA (termed miR-neg) were purchased from Shanghai GenePharma (Shanghai, China). miRNA inhibitor of miR-3664-3p and a negative control were purchased from Ambion (Applied Biosystems, CA, US). Total RNA samples from a panel of human tissues were purchased from Ambion (FirstChoice® Human Total RNA Survey Panel, Applied Biosystems, CA, US). The normal human liver tissues were previously reported (Hu et al., 2014a).

Cell Transfection, RNA Extraction, and Reverse-Transcriptase Quantitative Real-Time Polymerase Chain Reaction (RT-qPCR). HepG2 cells were obtained from the American Type Culture (ATCC) and HuH7 cells were obtained from Dr. Jillian Carr (Flinders University, Adelaide, Australia). Both cell lines were maintained in Dulbecco's modified Eagles's medium (DMEM) containing 10% (v/v) fetal bovine serum (FBS) at 37°C in a 5% CO_2 atmosphere. Cells were plated in 6-well plates and cultured overnight reaching 60 to 70% confluence prior to transfection. Transfections were performed with miRNA-mimics, miRNA-inhibitor or miR-neg in triplicate at 30 nM using 8 µl Lipofectamine 2000 (Invitrogen) per well. Total RNA was extracted after 24 hours using TRIzol reagent according to the manufacturer's protocol (Invitrogen). The expression levels of target genes (*UGT2B7*, *UGT2B4*, *18S rRNA* and *GAPDH*) were quantified using reverse-transcriptase quantitative real-time polymerase chain reaction (RT-qPCR) in a RotorGene 3000 instrument

Downloaded from jpet.aspetjournals.org at ASPET Journals on March 20, 2024

JPET Fast Forward. Published on April 7, 2017 as DOI: 10.1124/jpet.116.239707
This article has not been copyedited and formatted. The final version may differ from this version.

(Corbett Research, NSW, Australia) as previously reported (Hu et al., 2010, Hu and Mackenzie, 2009, Hu and Mackenzie, 2010). Quantification of miRNAs (miR3664-3p, miR-135a-5p, miR-410-3p miR-1266-5p, miR-4483, miR-4317, miR216b-5p, miR-489-3p, miR-4691-5p, miR-101-3p) and RNU6-2 (miR-U6 small nuclear-2 RNA as a house-keeping miRNA) was performed as previously reported (Balcells et al., 2011, Wijayakumara et al., 2015). The expression levels of target genes relative to 18S rRNA were quantified using the $2^{-\Delta\Delta}$CT method (Livak and Schmittgen, 2001). The expression levels of individual miRNAs were presented relative to that of RNU6-2 (set as a value of 100%). Primers for RT-qPCR of miRNAs are listed in Table 1.

Generation of Luciferase Reporter Constructs and Mutagenesis. The UGT2B7 mRNA (NM_001074.3) contains a 251-base pair (bp) 3'-untranslated region (UTR), whereas the UGT2B4 mRNA (NM_021139.2) contains a 469-bp 3'-UTR. The full-length UGT2B7 3'-UTR region between the stop codon (TAG) and the poly (A) tail was amplified from human genomic DNA (Roche Diagnostic, Indianapolis, IN) using Phusion hot-start high-fidelity DNA polymerase (Thermo Fisher Scientific, Pittsburgh, PA), and cloned into the XbaI restriction site of the pGL3-promoter vector (Promega), generating the reporter construct pGL3/2B7/UTR. Similarly, the full-length UGT2B4 3'-UTR region between the stop codon and the poly (A) tail was amplified and cloned into the pGL3-promoter vector, generating the reporter construct pGL3/2B4/UTR. Primers used for amplifying the 3'-UTR of UGT2B4 or UGT2B7 are listed in Table 1.

Using the pGL3/2B7/UTR construct as a template and the QuickChange site-directed mutagenesis kit (Stratagene, La Jolla, CA), the UGT2B7 miR-3664-3p seed site (5'-U<u>CCUG</u>AG-3'), which is complementary to the miR-3664-3p seed sequence (3'-AGGACUC-5'), was changed to 5'-U<u>AGCU</u>AG-3' producing the mutated construct

Downloaded from jpet.aspetjournals.org at ASPET Journals on March 20, 2024

JPET Fast Forward. Published on April 7, 2017 as DOI: 10.1124/jpet.116.239707
This article has not been copyedited and formatted. The final version may differ from this version.

pGL3/2B7/UTR/miR-3664/MT. Similarly, using the pGL3/2B4/UTR construct as template, the UGT2B4 miR-135a-5p seed site was mutated from 5'-AAAGCCAU-3' to 5'-AAAUGACU-3', generating the mutated construct pGL3/2B4/UTR/miR-135a/MT; the UGT2B4 miR-410-3p seed site was mutated from 5'-GUUAUAU-3' to 5'-GUCCGCU-3', generating the mutated construct pGL3/2B4/UTR/miR-410/MT. The identities of all constructs were confirmed by DNA sequencing. Primers used for mutagenesis are listed in Table 1.

Luciferase reporter assays. HepG2 and HuH7 cells were plated in 96-well plates and cultured overnight prior to transfection. Transfection was conducted in quadruplicate for each condition; each well was transfected with 100 ng of each UTR luciferase reporter, 0.8 ng of pRL-null vector and 30 nM miRNA-mimics of each miRNA or miR-neg as the negative control. 24 hours post transfection, cells were lysed in passive lysis buffer, and then subjected to Dual-Luciferase Reporter Assay according to the manufacturer's instructions (Promega, Madison, WI). Firefly and Renilla luciferase activities were measured using a Packard TopCount luminescence and scintillation counter (PerkinElmer Life and Analytical Sciences, Waltham, MA). Firefly luciferase activity was first normalized to Renilla activity and the reporter activity was then presented relative to that of the control pGL3-promoter vector (set at a value of 100%).

Western Blotting. HepG2 cells were transfected with miRNA mimics (miR-3664-3p or miR-neg) at 30 nM and 72 hours post-transfection, whole cell lysates were prepared with RIPA buffer (50 mM Tris–HCl, pH 7.4, 150 mM NaCl, 1% NP-40, 2 mM EDTA, 0.5% sodium deoxycholate, 0.1% sodium dodecyl sulphate). Protein concentrations of cell lysates were measured using the Bradford Protein Assay (Bio-Rad, Hercules, CA). Fifty micro-

Downloaded from jpet.aspetjournals.org at ASPET Journals on March 20, 2024

JPET Fast Forward. Published on April 7, 2017 as DOI: 10.1124/jpet.116.239707
This article has not been copyedited and formatted. The final version may differ from this version.

grams of each cell lysate were subjected to SDS-polyacrylamide gel electrophoresis on 12% acrylamide gels and transferred onto nitrocellulose membranes. The anti-UGT2B7 antibody used in western blotting was developed in our laboratory as previously reported (Hu et al., 2014c). After the membranes were probed with primary antibodies (anti-UGT2B7 or anti-Calnexin [Sigma Aldrich]), the membranes were probed with horseradish peroxidase-conjugated donkey anti-rabbit secondary antibody (NeoMarkers). SuperSignal®West Pico Chemiluminescent kit (Thermo Fisher Scientific) and the LAS4000 luminescent image analyzer (GE Healthcare Life Sciences, Piscataway, NJ) were used for visualizing immunosignals. Band intensity was quantified using Multi Gauge Version 3.0 image software (FUJIFILM, Tokyo, Japan).

Morphine Glucuronidation Assay. HepG2 cells were plated in 6-well plates and cultured overnight before the transfection with mimics (miR-neg or miR-3664-3p) at 30 nM. Whole cell lysates were prepared after 24 hours post-transfection with 80 µl of TE buffer (10 mM Tris-HCl, 1 mM EDTA, pH 7.6) and the protein concentrations of the lysates were determined as described above. A 200-µl reaction of each sample containing 100 mM potassium phosphate pH 7.4, 4 mM $MgCl_2$, 5 mM morphine, 125 µg lysate protein and 5 mM UDPGA, were incubated for 2 hours at 37^{o}C in a shaking water bath. The glucuronidation reaction was terminated by the addition of 2 µl of 70% (v/v) perchloric acid and samples were kept on ice for 30 minutes before centrifugation at 5000g for 10 minutes at 4°C. The supernatant fraction (~40 µl) was analysed by high-performance liquid chromatography (HPLC) using an Agilent 1100 series instrument (Agilent Technologies, Sydney, Australia) as previously described (Uchaipichat et al., 2004). The HPLC column eluent was monitored by fluorescence detection at an excitation wavelength of 235nm and an emission wavelength of 345 nm. Quantification of morphine-3-glucuronide concentrations in the samples were

Downloaded from jpet.aspetjournals.org at ASPET Journals on March 20, 2024

JPET Fast Forward. Published on April 7, 2017 as DOI: 10.1124/jpet.116.239707
This article has not been copyedited and formatted. The final version may differ from this version.

calculated by comparing peak areas of the samples to those of standard curves prepared over the concentration ranges of 0.5 to 40 μM morphine-3-glucuronide. Morphine-6-glucuronide concentration was not detected in the samples.

Data Analyses of Liver Hepatocellular Carcinoma (TCGA-LIHC). Transcriptome profiling data of RNAseq and miRNAseq of Liver Hepatocellular Carcinoma (LIHC) were downloaded from The Cancer Genome Atlas (TCGA) data portal (https://gdc-portal.nci.nih.gov/). The LIHC RNAseq expression data from 371 samples were represented in the form of HTSeq-counts. Genes (protein coding and non-coding) with less than a mean of 10 counts were discarded; the counts of the remaining genes were normalized using Upper Quantile normalization method. Correlation analyses between the expression levels of UGT and miRNA gene sets were conducted using Spearman's rank method and plots were drawn using statistical package R (https://cran.r-project.org/).

Statistical Analysis. Statistical analysis of all data was performed using GraphPad Prism 6 software (La Jolla, CA, USA), with a two-tailed Student's independent t-test. Correlation analyses between expression levels of a UGT gene and a miRNA in the panel of liver tissues or the panel of human tissues were conducted by Spearman correlation. A p value of < 0.05 was considered statistically significant.

Results

The 3'-UTRs of UGT2B7 and UGT2B4 Contain Putative miRNA Target Sites. Our sequence analysis of UGT2B7 3'-UTR using TargetScan software (www.targetscan.org) identified putative target sites for 5 miRNAs, namely miR-3664-3p, miR-1266-5p, miR-4483,

Downloaded from jpet.aspetjournals.org at ASPET Journals on March 20, 2024

JPET Fast Forward. Published on April 7, 2017 as DOI: 10.1124/jpet.116.239707
This article has not been copyedited and formatted. The final version may differ from this version.

miR-4317, and miR-216b-5p (Supplemental Fig. 1A). To test the potential functionalities of these sites, we cloned the UGT2B7 3'-UTR into the pGL3 vector downstream of the luciferase gene, generating the UGT2B7 3'-UTR luciferase reporter (termed pGL3/2B7/UTR). Co-transfection of pGL3/2B7/UTR with miRNA mimics targeting the 5 predicted binding sites in HepG2 cells showed that two of the five mimics, namely miR-3664-3p and miR-216b-5p mimics, significantly reduced the reporter activity by 51% and 22%, respectively (Fig. 1A).

Our sequence analysis of the UGT2B4 3'-UTR using the TargetScan software predicted putative target sites for 6 microRNAs, namely: miR-135a-5p, miR-410-3p, miR-489-3p, miR-4691-5p, miR-216b-5p, and miR-101-3p (Supplemental Fig. 1B). We cloned the UGT2B4 3'-UTR into the pGL3 vector downstream of the luciferase gene, generating the UGT2B4 3'-UTR luciferase reporter (termed pGL3/2B4/UTR). Co-transfection of pGL3/2B4/UTR with miRNA mimics targeting the 6 predicted binding sites in HepG2 cells showed that the reporter activity was significantly reduced by 39%, 30%, 22%, 24% and 24% by miR-135a-5p, miR-410-3p, miR-489-3p, miR-4691-5p and miR-216b-5p, respectively (Fig. 1B). miR-101-3p mimics did not alter the reporter activity (Fig. 1B). The expression levels of the above-mentioned 10 miRNAs in HepG2 cells were measured by quantitative real-time PCR. As shown in Fig. 1C, miR-135a-5p and miR-101-3p were highly expressed; however, four miRNAs (miR-3664-3p, miR-1266-5p, miR-4317, miR-410-3p) were expressed at relatively low levels, and the remaining four miRNAs (miR-4483, miR-216b-5p, and miR-489-3p, miR-4691-5p) were not detectable. The downregulation of *UGT2B4* and *UGT2B7* by miR-216b-5p in liver cancer cell lines was recently reported (Dluzen et al., 2016). In the present study, we define the roles of miR-3664-3p, miR-135a-5p, and miR-410-3p in regulation of *UGT2B4* and *UGT2B7* in liver cancer cell lines.

Downloaded from jpet.aspetjournals.org at ASPET Journals on March 20, 2024

JPET Fast Forward. Published on April 7, 2017 as DOI: 10.1124/jpet.116.239707
This article has not been copyedited and formatted. The final version may differ from this version.

Regulation of UGT2B7 by miR-3664-3p in Liver Cancer Cell Lines.

The predicted miR-3664-3p binding site in the *UGT2B7* 3'UTR is located at nucleotides 77-99 downstream of the *UGT2B7* stop codon (Fig. 2A). This site is defined as a 8mer site by TargetScan (pairing to the 2–7 nt miRNA seed and nucleotide 8 plus an A at nucleotide 1), and also shows 3'-sequence pairing of nucleotides 11-15 to miR-3664-3p. A 3'-sequence pairing at nucleotides 12–17 of miRNAs has been shown to enhance the efficacy of miRNA targeting (Grimson et al., 2007). To show a direct role of this site in the miR-3664-3p mimic-mediated reduction in pGL3/2B7/UTR reporter activity, the miR-3664-3p site in the pGL3/2B7/UTR reporter was mutated generating the construct pGL3/2B7/UTR/miR3664/MT (Fig. 2B). miR-3664-3p mimics were co-transfected with wild-type pGL3/2B7/UTR or pGL3/2B7/UTR/miR3664/MT reporter into HepG2 and HuH7 cells. The miR-3664-3p mimics significantly reduced the activity of the wild-type reporter in both cell lines; this reduction was abolished in HepG2 cells (Fig. 2C) or significantly abrogated in HuH7 cells (Fig. 2D) by a mutation of the miR-3664-3p site. These results indicate that *UGT2B7* is a direct target of miR-3664-3p in HepG2 and HuH7 cells.

The impact of miR-3664-3p on the expression and activity of UGT2B7 was tested in HepG2 cells using miRNA mimics and inhibitors. As expected, miR-3664-3p mimics significantly reduced the UGT2B7 mRNA levels and miR-3664-3p inhibitor significantly increased the UGT2B7 mRNA levels in HepG2 cells (Fig. 3A), while GAPDH mRNA levels were not significantly altered (Fig. 3B). Western blotting with a UGT2B7-specific antibody (Hu et al., 2014c) showed that UGT2B7 protein levels were reduced by 28% in HepG2 cells transfected with miR-3664-3p mimics relative to the miR-neg control (Fig. 3C). UGT2B7 glucuronidation activity was tested by HPLC assay using morphine as a substrate. There was a significant 41% reduction in morphine glucuronidation in HepG2 cells transfected with miR-3664-3p mimics relative to the miR-neg control (Fig. 3D). Collectively, these data

Downloaded from jpet.aspetjournals.org at ASPET Journals on March 20, 2024

JPET Fast Forward. Published on April 7, 2017 as DOI: 10.1124/jpet.116.239707
This article has not been copyedited and formatted. The final version may differ from this version.

define a novel miR-3664-3p target site in the UGT2B7 3'-UTR that negatively regulates UGT2B7 expression and activity in liver cancer cell lines.

To assess whether miR-3664-3p might play a role inof the expression of UGT2B7 in normal liver, we measured the expression levels of miR-3664-3p and UGT2B7 in a panel of 18 normal human liver tissues using RT-qPCR. Consistent with previous reports (Congiu et al., 2002, Court, 2010), UGT2B7 mRNA levels were very high in liver tissues. In contrast, levels of miR-3664-3p were extremely low or undetectable (data not shown). An analysis of RNA-seq data from a cohort of 371 liver hepatocellular carcinomas (LIHC) from The Cancer Genome Atlas (TCGA) also revealed high levels of UGT2B7 mRNA and extremely low levels of miR-3664 (data not shown). These observations suggest a negative correlation between miR-3664 and UGT2B7 mRNA levels in both normal and cancerous liver tissues. Although an overall correlation analysis between miR-3664 and UGT2B7 mRNA levels in liver cancer/liver tissue was not possible due to the lack of miR-3664 expression in most samples, we did measure a significant negative correlation between the expression levels of UGT2B7 and miR-3664-3p in a panel of 10 normal human tissues that did express both UGT2B7 and miR-3664-3p (liver, kidney, colon, small intestine, ovary, testis, trachea, lung, thyroid, placenta) (Pearson's r-0.80, $p<0.001$) (Fig. 3E).

Regulation of UGT2B4 by miR-135a-5p and miR-410-3p in Liver Cancer Cell Lines.

The predicted miR-135a-5p binding site in the *UGT2B4* 3'UTR is located at nucleotides 202-224 downstream of the stop codon and is defined as an 8mer site by Targetscan (Fig. 2B). In addition to the seed pairing the miR-135a-5p binding site has 3'-sequence pairing to miR-135a-5p (Fig. 4A). The predicted miR-410-3p binding site is located

Downloaded from jpet.aspetjournals.org at ASPET Journals on March 20, 2024

JPET Fast Forward. Published on April 7, 2017 as DOI: 10.1124/jpet.116.239707
This article has not been copyedited and formatted. The final version may differ from this version.

at nucleotides 213-235 downstream of the UGT2B4 stop codon and is defined as a 7mer-m8 site (pairing to the 2-7 nt miRNA seed and nucleotide 8). The miR-410-3p binding site also has substantial 3'-sequence pairing to miR-410-3p including nt 13-17 (Fig. 4A). Of note, the 5' 11 nucleotides (5'AUAAAGCCAUA3') of miR-135a-5p target site overlap with the 3' 11 nucleotides of miR-410-5p target site in the UGT2B4 3'-UTR (Supplemental Figure 1B). To investigate the regulation of *UGT2B4* by miR-135a-5p and miR-410-3p through these two predicted sites, we mutated the sites in the pGL3/2B4/UTR reporter construct to generate the pGL3/2B4/UTR/miR135a/MT and pGL3/2B4/UTR/miR410/MT constructs (Fig. 4B). Co-transfection of miR-135a-5p mimics with the reporter constructs showed that miR-135a-5p significantly decreased the activity of the wild-type reporter but did not significantly alter the activity of pGL3/2B4/UTR/miR135a/MT in both HepG2 (Fig. 4C) and HuH7 (Fig. 4D) cells. Co-transfection of miR-410-3p mimics with the reporters showed that miR-410-3p significantly reduced the activity of the wild-type reporter but not that of pGL3/2B4/UTR/miR410/MT in HepG2 cells (Fig. 4D).

To assess the these miRNAs in regulation of endogenous UGT2B4 mRNA levels, we transfected microRNA mimics targeting miR-135a-5p or miR-410-3p in HuH7 cells, these cells were used because they had higher levels of UGT2B4 expression relative to HepG2 cells (see Supplemental Figure 2). Both miR-135a-5p and miR-410-3p mimics significantly reduced UGT2B4 mRNA levels (Fig. 5A) but did not change GAPDH mRNA levels (Fig. 5B). Collectively, these results indicate that *UGT2B4* is a direct target of miR-135a-5p and miR-410-3p in liver cancer cells. However, the potential impact of these miRNAs on UGT2B4 protein level or enzymatic activity could not be assessed due to the lack of a UGT2B4-specific antibody or a probe substrate that would be specific for UGT2B4 in HepG2 or HuH7 cells.

Downloaded from jpet.aspetjournals.org at ASPET Journals on March 20, 2024

JPET Fast Forward. Published on April 7, 2017 as DOI: 10.1124/jpet.116.239707
This article has not been copyedited and formatted. The final version may differ from this version.

The relationship between miR-135a-5p and UGT2B4 expression levels was assessed in a panel of 18 normal human liver tissues using quantitative real-time PCR, revealing a significant negative correlation (Spearman r = -0.47, p = 0.047) (Fig. 5C). We also measured miR-135a-5p and UGT2B4 levels in HepG2 and Huh7 cells and found that miR-135a-5p levels are significantly lower in Huh7 cells than in HepG2 cells, while conversely UGT2B4 levels are significantly higher in Huh7 cells than in HepG2 cells (Supplemental Fig 2), suggesting that negative correlation extends to these liver cancer cell lines. In contrast, when we examined miR-135a and UGT2B4 levels in the TCGA-LIHC RNA-seq dataset containing 371 hepatocellular carcinoma specimens, we saw no correlation (Supplemental Figure 3). Finally, we measured miR-135a-5p and UGT2B4 levels in in a panel of 10 normal human tissues (liver, kidney, colon, small intestine, ovary, testis, trachea, lung, thyroid, placenta). Both genes varied widely in expression but were uncorrelated (data not shown).

.

No correlation was observed between UGT2B4 and miR-410-3p expression levels in the normal human liver tissue panel (data not shown). However, analysis of the TCGA-LIHC RNA-seq dataset (371 hepatocellular carcinoma specimens) revealed a significant negative correlation between miR-410 and UGT2B4 mRNA levels (Spearman r = -0.15, p = 0.002) (Fig. 5D). Furthermore, we also observed a significant negative correlation between the expression levels of UGT2B4 and miR-410-3p in the panel of 10 normal human tissues (liver, kidney, testis, lung, thyroid, placenta, prostate, heart, cervix) (Pearson's r = -0.76, p = 0.010) (Fig. 5E).

Discussion

Downloaded from jpet.aspetjournals.org at ASPET Journals on March 20, 2024

JPET Fast Forward. Published on April 7, 2017 as DOI: 10.1124/jpet.116.239707
This article has not been copyedited and formatted. The final version may differ from this version.

UGT2B4 and *UGT2B7* are highly expressed in the liver. While their transcriptional regulation has been well studied (Hu et al., 2014b), to date there has been only one report of their post-transcriptional regulation by miR-216b-5p in liver cancer cell lines (Dluzen et al., 2016). We used bioinformatics analysis to predict multiple potential miRNA binding sites in the UGT2B7 and UGT2B4 3'-UTRs, and were able to confirm a subset of these experimentally. In particular, we used reporter analysis, mutagenesis, and endogenous gene expression analysis to show that miR-3664-3p negatively regulates the UGT2B7 mRNA via a binding site in the 3'UTR. We also showed inhibition of UGT2B7 at both protein and activity levels using a specific antibody and probe substrate. Similarly, we found that miR-135a-5p and miR-410-3p bind and regulate the UGT2B4 mRNA. Both miR-410 (Marrone et al., 2016, Wang et al., 2014) and miR-135a (Liu et al., 2012, Zeng et al., 2016) are reported to be upregulated in liver cancer and are considered as liver oncomiRs. By contrast, these two miRNAs are frequently downregulated in some other cancers including breast, prostate and pancreatic cancer (Chien et al., 2011, Gattolliat et al., 2011, Theodore et al., 2014, Tang et al., 2014). Overexpression of miR-3664 in the peripheral blood of glioblastoma patients (Dong et al., 2014) and gastric cancer (Liu et al., 2014) was recently reported; however, the biological role of miR-3664-3p in liver cancer remains to be investigated.

miRNAs generally repress gene expression through mRNA degradation or translational repression depending on the degree and nature of sequence complementarity between the miRNA guide and mRNA target (Macfarlane and Murphy, 2010). Extensive base-pairing between the miRNA guide and mRNA target permits mRNA cleavage by Argonaute (Ago2) (Macfarlane and Murphy, 2010); expression levels of such miRNAs and their targets may thus be negatively correlated due to miRNA-mediated mRNA degradation. The three functional miR-binding sites (UGT2B4 miR-135a-5p, UGT2B4 miR-410-3p, and UGT2B7 3664-3p) reported in the present study showed (Fig. 2A and Fig. 4A) extensive

Downloaded from jpet.aspetjournals.org at ASPET Journals on March 20, 2024

JPET Fast Forward. Published on April 7, 2017 as DOI: 10.1124/jpet.116.239707
This article has not been copyedited and formatted. The final version may differ from this version.

seed-pairing and additional 3'-sequence pairing (s) with their targets, which would be expected to favour the mRNA degradation pathway.

Given the predicted role of each of the miRNAs that we studied in target mRNA degradation, we further predicted that negative correlations might be observed between miRNA levels and target mRNA levels in various tissues. While this was the case for some of our miRNA-mRNA pairings, it was not necessarily seen in all of the contexts examined. Moreover when interpreting our data it is important to consider that correlation alone does not imply causation, and many regulatory factors, both transcriptional and post-transcriptional, are involved in the regulation of a given gene. In the case of miR-3664 and UGT2B7, levels were negatively correlated in both normal and cancerous liver tissues with high expression of *UGT2B7* and low (or absent) expression of miR-3664. One reasonable interpretation of this result is that the absence (or very low level) of miR-3664 *permits* a high steady state level of UGT2B7 mRNA to be maintained. However, this causal relationship would need to be explicitly tested in order to state definitively that miR-3664-3p is an important endogenous regulator of basal UGT2B7 levels. Interestingly, in the analysis of the 10-tissue panel (including 9 extrahepatic tissues), whilst UGT2B7 and miR-3664-3p levels were still negatively correlated overall, there were some tissues with low or absent UGT2B7 levels (ovary, trachea, and testis) that also had very low miR-3664-3p levels. This may be explained by considering the role of transcriptional (promoter level) regulation in determining the overall level of UGT2B7 expression. The key positive transcriptional regulators that activate the UGT2B7 promoter in liver (e.g. HNFs) have little activity in tissues such as trachea, ovary and testis, hence we expect low or absent UGT2B7 transcription. In this context, posttranscriptional regulation may have little relevance.

We found a negative correlation between miR-410 and UGT2B4 mRNA levels in the liver cancer TCGA cohort of 371 specimens as well as in the panel of 10 normal human

Downloaded from jpet.aspetjournals.org at ASPET Journals on March 20, 2024

JPET Fast Forward. Published on April 7, 2017 as DOI: 10.1124/jpet.116.239707
This article has not been copyedited and formatted. The final version may differ from this version.

tissues, but unexpectedly, not in the panel of 18 normal livers. This discrepancy remains to be resolved and may be clarified in the future by examining larger cohorts of normal livers and liver cancers.

The relationship between miR-135a and UGT2B4 mRNA levels in the various samples that we analysed was also complex. Although there was a negative correlation in the panel of 18 normal livers, there was no correlation between the levels of these genes in the liver cancer TCGA cohort. This could be related to deregulation of other miRNAs and transcription factors that are involved in controlling UGT2B4 expression in liver cancer (Callegari et al., 2015, Negrini et al., 2011). Of note, Dluzen et al recently reported the regulation of three *UGT1A* genes (1A1, 1A3, 1A6) by miR-491-3p in liver cancer cells and a significant inverse correlation between miR-491-3p and mRNA levels of UGT1A3 and UGT1A6 (but not UGT1A1) in a panel of normal human liver specimens (Dluzen et al., 2014).

Several studies have investigated the cooperative regulation of single target mRNAs by multiple miRNAs and revealed that the efficacy and cooperativity between miRNA target sites is predominantly determined by the interval spacing between seed sites (Doench and Sharp, 2004, Grimson et al., 2007, Pasquinelli, 2012, Saetrom et al., 2007). Specifically, the most effective cooperative down-regulation is seen when the distance of two seed sites is between 13 and 35 nucleotides (nt); however, this cooperativity becomes less likely when the internal spacing between miRNA seed sites is over 70 nt (Saetrom et al., 2007). The seed site is defined as nucleotides 2-8 from the 3' end of a miRNA target site that are normally complementary to the seed sequence of the cognate miRNA (Bartel, 2009). Our findings together with the recent report by Dluzen (Dluzen et al., 2016) indicate that *UGT2B4* is a direct target of three miRNAs (miR-135a-5p, miR-410-3p, miR-216b-5p). As mentioned earlier, the 5' 11 nucleotides of miR-135a-5p site overlap with the 3' 11 nucleotides of miR-

Downloaded from jpet.aspetjournals.org at ASPET Journals on March 20, 2024

JPET Fast Forward. Published on April 7, 2017 as DOI: 10.1124/jpet.116.239707
This article has not been copyedited and formatted. The final version may differ from this version.

410-3p site in the UGT2B4 3'-UTR (Supplemental Fig. 1B). The seed sites of these two miRNAs are separated by 12 nt, which falls just outside of the proposed optimal spacing range; whether miR-135a-5p and miR-410-3p could cooperatively regulate *UGT2B4* remains to be investigated in future studies. The miR-135a-5p site (or miR-410-3p site) and miR-216b-5p site is separated by 137 nt (or 149 nt) in the UGT2B4 3'-UTR (Supplemental Fig. 1B), and the miR-3664-3p site and the recently reported miR-216-5p site (Dluzen et al., 2016) are 73 nt apart in the UGT2B7 3'-UTR (Supplemental Fig. 1A). Therefore, the cooperativity between these miRNA target sites is predicted to be less likely; however this also remains to be tested.

When initially screening the predicted miRNA binding sites using luciferase reporters, we also found repression of the UGT2B4 3'-UTR reporter by miR-4691-5p and miR-489-3p (Fig. 1B). The putative binding sites for miR-4691-5p and miR-489-3p in the UGT2B4 3' UTR include overlapping seed sequences (Supplemental Fig. 1B). Thus miR-4691-5p and miR-489-3p could possibly inhibit each other's activity based on a model of competitive loading of miRNA-activated miRISCs (miRNA-induced silencing complexes) (Macfarlane and Murphy, 2010), In contrast, cooperative regulation between the miR-135a-3p and miR-4691-5p (or miR-489-3p) target sites may be possible as the spacing between their seed sites is within the optimal range (13-35 nt) for cooperativity. Again future studies are required to test these possibilities.

In summary, the present study demonstrates that UGT2B4 is a direct target of miR-135a-5p and miR-410-3p and that UGT2B7 is a direct target of miR-3664-3p in liver cancer cells. Combined with other recent reports of miRNA-mediated UGT regulation (Dluzen et al., 2014, Dluzen et al., 2016, Wijayakumara et al., 2015, Margaillan et al., 2016), our observations suggest that post-transcriptional regulation of UGTs by miRNAs may have an important role in fine-tuning glucuronidation activity in the liver as well as extrahepatic

Downloaded from jpet.aspetjournals.org at ASPET Journals on March 20, 2024

JPET Fast Forward. Published on April 7, 2017 as DOI: 10.1124/jpet.116.239707
This article has not been copyedited and formatted. The final version may differ from this version.

tissues. While none of the miRNAs characterized in this study are predicted to have a role in cancer-specific UGT regulation, further analysis of the functional significance of the miRNA-regulatory network is ongoing. In particular, it is interesting to consider whether deregulation of miRNA expression due to cellular stress or inflammation could alter UGT levels and hence the capacity for detoxification, which in turn may impact on cancer risk.

Downloaded from jpet.aspetjournals.org at ASPET Journals on March 20, 2024

JPET Fast Forward. Published on April 7, 2017 as DOI: 10.1124/jpet.116.239707
This article has not been copyedited and formatted. The final version may differ from this version.

Authorship Contributions

Participated in research design: Meech, Hu, Mackenzie, Wijayakumara.

Conducted experiments: Wijayakumara.

Performed data analysis: Wijayakumara, Hu, Meech, Mackenzie.

Wrote or contributed to the writing of the manuscript: Meech, Hu, Wijayakumara, Mackenzie, McKinnon.

Downloaded from jpet.aspetjournals.org at ASPET Journals on March 20, 2024

JPET Fast Forward. Published on April 7, 2017 as DOI: 10.1124/jpet.116.239707
This article has not been copyedited and formatted. The final version may differ from this version.

References

ARGIKAR, U. A. & REMMEL, R. P. 2009. Effect of aging on glucuronidation of valproic acid in human liver microsomes and the role of UDP-glucuronosyltransferase UGT1A4, UGT1A8, and UGT1A10. *Drug Metab Dispos,* 37**,** 229-36.

BALCELLS, I., CIRERA, S. & BUSK, P. K. 2011. Specific and sensitive quantitative RT-PCR of miRNAs with DNA primers. *BMC Biotechnol,* 11**,** 70.

BARBIER, O., DURAN-SANDOVAL, D., PINEDA-TORRA, I., KOSYKH, V., FRUCHART, J. C. & STAELS, B. 2003a. Peroxisome proliferator-activated receptor alpha induces hepatic expression of the human bile acid glucuronidating UDP-glucuronosyltransferase 2B4 enzyme. *J Biol Chem,* 278**,** 32852-60.

BARBIER, O., TORRA, I. P., SIRVENT, A., CLAUDEL, T., BLANQUART, C., DURAN-SANDOVAL, D., KUIPERS, F., KOSYKH, V., FRUCHART, J. C. & STAELS, B. 2003b. FXR induces the UGT2B4 enzyme in hepatocytes: a potential mechanism of negative feedback control of FXR activity. *Gastroenterology,* 124**,** 1926-40.

BARRE, L., FOURNEL-GIGLEUX, S., FINEL, M., NETTER, P., MAGDALOU, J. & OUZZINE, M. 2007. Substrate specificity of the human UDP-glucuronosyltransferase UGT2B4 and UGT2B7. Identification of a critical aromatic amino acid residue at position 33. *Febs j,* 274**,** 1256-64.

BARTEL, D. P. 2009. MicroRNAs: target recognition and regulatory functions. *Cell,* 136**,** 215-33.

CALLEGARI, E., GRAMANTIERI, L., DOMENICALI, M., D'ABUNDO, L., SABBIONI, S. & NEGRINI, M. 2015. MicroRNAs in liver cancer: a model for investigating pathogenesis and novel therapeutic approaches. *Cell Death Differ,* 22**,** 46-57.

CHIEN, W. W., DOMENECH, C., CATALLO, R., KADDAR, T., MAGAUD, J. P., SALLES, G. & FFRENCH, M. 2011. Cyclin-dependent kinase 1 expression is inhibited by p16(INK4a) at the post-transcriptional level through the microRNA pathway. *Oncogene,* 30**,** 1880-91.

COFFMAN, B. L., RIOS, G. R., KING, C. D. & TEPHLY, T. R. 1997. Human UGT2B7 catalyzes morphine glucuronidation. *Drug Metab Dispos,* 25**,** 1-4.

CONGIU, M., MASHFORD, M. L., SLAVIN, J. L. & DESMOND, P. V. 2002. UDP glucuronosyltransferase mRNA levels in human liver disease. *Drug Metab Dispos,* 30**,** 129-34.

COURT, M. H. 2010. Interindividual variability in hepatic drug glucuronidation: studies into the role of age, sex, enzyme inducers, and genetic polymorphism using the human liver bank as a model system. *Drug Metab Rev,* 42**,** 209-24.

DLUZEN, D. F., SUN, D., SALZBERG, A. C., JONES, N., BUSHEY, R. T., ROBERTSON, G. P. & LAZARUS, P. 2014. Regulation of UDP-glucuronosyltransferase 1A1 expression and activity by microRNA 491-3p. *J Pharmacol Exp Ther,* 348**,** 465-77.

DLUZEN, D. F., SUTLIFF, A., CHEN, G., WATSON, C., ISHMAEL, F. T. & LAZARUS, P. 2016. Regulation of UGT2B expression and activity by miR-216b in liver cancer cell lines. *J Pharmacol Exp Ther*.

DOENCH, J. G. & SHARP, P. A. 2004. Specificity of microRNA target selection in translational repression. *Genes Dev,* 18**,** 504-11.

DONG, L., LI, Y., HAN, C., WANG, X., SHE, L. & ZHANG, H. 2014. miRNA microarray reveals specific expression in the peripheral blood of glioblastoma patients. *Int J Oncol,* 45**,** 746-56.

FOURNEL-GIGLEUX, S., JACKSON, M. R., WOOSTER, R. & BURCHELL, B. 1989. Expression of a human liver cDNA encoding a UDP-glucuronosyltransferase

Downloaded from jpet.aspetjournals.org at ASPET Journals on March 20, 2024

JPET Fast Forward. Published on April 7, 2017 as DOI: 10.1124/jpet.116.239707
This article has not been copyedited and formatted. The final version may differ from this version.

catalysing the glucuronidation of hyodeoxycholic acid in cell culture. *FEBS Lett,* 243**,** 119-22.

GATTOLLIAT, C. H., THOMAS, L., CIAFRE, S. A., MEURICE, G., LE TEUFF, G., JOB, B., RICHON, C., COMBARET, V., DESSEN, P., VALTEAU-COUANET, D., MAY, E., BUSSON, P., DOUC-RASY, S. & BENARD, J. 2011. Expression of miR-487b and miR-410 encoded by 14q32.31 locus is a prognostic marker in neuroblastoma. *Br J Cancer,* 105**,** 1352-61.

GREGORY, P. A., GARDNER-STEPHEN, D. A., ROGERS, A., MICHAEL, M. Z. & MACKENZIE, P. I. 2006. The caudal-related homeodomain protein Cdx2 and hepatocyte nuclear factor 1alpha cooperatively regulate the UDP-glucuronosyltransferase 2B7 gene promoter. *Pharmacogenet Genomics,* 16**,** 527-36.

GRIMSON, A., FARH, K. K., JOHNSTON, W. K., GARRETT-ENGELE, P., LIM, L. P. & BARTEL, D. P. 2007. MicroRNA targeting specificity in mammals: determinants beyond seed pairing. *Mol Cell,* 27**,** 91-105.

GUILLEMETTE, C. 2003. Pharmacogenomics of human UDP-glucuronosyltransferase enzymes. *Pharmacogenomics J,* 3**,** 136-58.

HU, D. G., GARDNER-STEPHEN, D., SEVERI, G., GREGORY, P. A., TRELOAR, J., GILES, G. G., ENGLISH, D. R., HOPPER, J. L., TILLEY, W. D. & MACKENZIE, P. I. 2010. A Novel Polymorphism in a Forkhead Box A1 (FOXA1) Binding Site of the Human UDP Glucuronosyltransferase 2B17 Gene Modulates Promoter Activity and Is Associated with Altered Levels of Circulating Androstane-3α,17β-diol Glucuronide. *Molecular Pharmacology,* 78**,** 714-722.

HU, D. G. & MACKENZIE, P. I. 2009. Estrogen receptor alpha, fos-related antigen-2, and c-Jun coordinately regulate human UDP glucuronosyltransferase 2B15 and 2B17 expression in response to 17beta-estradiol in MCF-7 cells. *Mol Pharmacol,* 76**,** 425-39.

HU, D. G. & MACKENZIE, P. I. 2010. Forkhead Box Protein A1 Regulates UDP-Glucuronosyltransferase 2B15 Gene Transcription in LNCaP Prostate Cancer Cells. *Drug Metabolism and Disposition,* 38**,** 2105-2109.

HU, D. G., MEECH, R., LU, L., MCKINNON, R. A. & MACKENZIE, P. I. 2014a. Polymorphisms and haplotypes of the UDP-glucuronosyltransferase 2B7 gene promoter. *Drug Metab Dispos,* 42**,** 854-62.

HU, D. G., MEECH, R., MCKINNON, R. A. & MACKENZIE, P. I. 2014b. Transcriptional regulation of human UDP-glucuronosyltransferase genes. *Drug Metab Rev,* 46**,** 421-58.

HU, D. G., ROGERS, A. & MACKENZIE, P. I. 2014c. Epirubicin upregulates UDP glucuronosyltransferase 2B7 expression in liver cancer cells via the p53 pathway. *Mol Pharmacol,* 85**,** 887-97.

INNOCENTI, F., IYER, L., RAMIREZ, J., GREEN, M. D. & RATAIN, M. J. 2001. Epirubicin glucuronidation is catalyzed by human UDP-glucuronosyltransferase 2B7. *Drug Metab Dispos,* 29**,** 686-92.

ISHII, Y., HANSEN, A. J. & MACKENZIE, P. I. 2000. Octamer transcription factor-1 enhances hepatic nuclear factor-1alpha-mediated activation of the human UDP glucuronosyltransferase 2B7 promoter. *Mol Pharmacol,* 57**,** 940-7.

JIN, C., MINERS, J. O., LILLYWHITE, K. J. & MACKENZIE, P. I. 1993. Complementary deoxyribonucleic acid cloning and expression of a human liver uridine diphosphate-glucuronosyltransferase glucuronidating carboxylic acid-containing drugs. *J Pharmacol Exp Ther,* 264**,** 475-9.

LEPINE, J., BERNARD, O., PLANTE, M., TETU, B., PELLETIER, G., LABRIE, F., BELANGER, A. & GUILLEMETTE, C. 2004. Specificity and regioselectivity of the

Downloaded from jpet.aspetjournals.org at ASPET Journals on March 20, 2024

JPET Fast Forward. Published on April 7, 2017 as DOI: 10.1124/jpet.116.239707
This article has not been copyedited and formatted. The final version may differ from this version.

conjugation of estradiol, estrone, and their catecholestrogen and methoxyestrogen metabolites by human uridine diphospho-glucuronosyltransferases expressed in endometrium. *J Clin Endocrinol Metab,* 89**,** 5222-32.

LEVESQUE, E., BEAULIEU, M., HUM, D. W. & BELANGER, A. 1999. Characterization and substrate specificity of UGT2B4 (E458): a UDP-glucuronosyltransferase encoded by a polymorphic gene. *Pharmacogenetics,* 9**,** 207-16.

LIU, D., HU, X., ZHOU, H., SHI, G. & WU, J. 2014. Identification of Aberrantly Expressed miRNAs in Gastric Cancer. *Gastroenterol Res Pract,* 2014**,** 473817.

LIU, S., GUO, W., SHI, J., LI, N., YU, X., XUE, J., FU, X., CHU, K., LU, C., ZHAO, J., XIE, D., WU, M., CHENG, S. & LIU, S. 2012. MicroRNA-135a contributes to the development of portal vein tumor thrombus by promoting metastasis in hepatocellular carcinoma. *J Hepatol,* 56**,** 389-96.

LIVAK, K. J. & SCHMITTGEN, T. D. 2001. Analysis of relative gene expression data using real-time quantitative PCR and the 2(-Delta Delta C(T)) Method. *Methods,* 25**,** 402-8.

LOUREIRO, A. I., FERNANDES-LOPES, C., BONIFACIO, M. J., WRIGHT, L. C. & SOARES-DA-SILVA, P. 2011. Hepatic UDP-glucuronosyltransferase is responsible for eslicarbazepine glucuronidation. *Drug Metab Dispos,* 39**,** 1486-94.

LU, Y., HEYDEL, J. M., LI, X., BRATTON, S., LINDBLOM, T. & RADOMINSKA-PANDYA, A. 2005. Lithocholic acid decreases expression of UGT2B7 in Caco-2 cells: a potential role for a negative farnesoid X receptor response element. *Drug Metab Dispos,* 33**,** 937-46.

MACFARLANE, L. A. & MURPHY, P. R. 2010. MicroRNA: Biogenesis, Function and Role in Cancer. *Curr Genomics,* 11**,** 537-61.

MACKENZIE, P. I., BOCK, K. W., BURCHELL, B., GUILLEMETTE, C., IKUSHIRO, S., IYANAGI, T., MINERS, J. O., OWENS, I. S. & NEBERT, D. W. 2005. Nomenclature update for the mammalian UDP glycosyltransferase (UGT) gene superfamily. *Pharmacogenet Genomics,* 15**,** 677-85.

MACKENZIE, P. I., OWENS, I. S., BURCHELL, B., BOCK, K. W., BAIROCH, A., BELANGER, A., FOURNEL-GIGLEUX, S., GREEN, M., HUM, D. W., IYANAGI, T., LANCET, D., LOUISOT, P., MAGDALOU, J., CHOWDHURY, J. R., RITTER, J. K., SCHACHTER, H., TEPHLY, T. R., TIPTON, K. F. & NEBERT, D. W. 1997. The UDP glycosyltransferase gene superfamily: recommended nomenclature update based on evolutionary divergence. *Pharmacogenetics,* 7**,** 255-69.

MARGAILLAN, G., LEVESQUE, E. & GUILLEMETTE, C. 2016. Epigenetic regulation of steroid inactivating UDP-glucuronosyltransferases by microRNAs in prostate cancer. *J Steroid Biochem Mol Biol,* 155**,** 85-93.

MARRONE, A. K., SHPYLEVA, S., CHAPPELL, G., TRYNDYAK, V., UEHARA, T., TSUCHIYA, M., BELAND, F. A., RUSYN, I. & POGRIBNY, I. P. 2016. Differentially expressed MicroRNAs provide mechanistic insight into fibrosis-associated liver carcinogenesis in mice. *Mol Carcinog,* 55**,** 808-17.

MAUL, R., WARTH, B., SCHEBB, N. H., KRSKA, R., KOCH, M. & SULYOK, M. 2014. In vitro glucuronidation kinetics of deoxynivalenol by human and animal microsomes and recombinant human UGT enzymes. *Arch Toxicol*.

NAKAMURA, A., NAKAJIMA, M., HIGASHI, E., YAMANAKA, H. & YOKOI, T. 2008. Genetic polymorphisms in the 5'-flanking region of human UDP-glucuronosyltransferase 2B7 affect the Nrf2-dependent transcriptional regulation. *Pharmacogenet Genomics,* 18**,** 709-20.

NEGRINI, M., GRAMANTIERI, L., SABBIONI, S. & CROCE, C. M. 2011. microRNA involvement in hepatocellular carcinoma. *Anticancer Agents Med Chem,* 11**,** 500-21.

Downloaded from jpet.aspetjournals.org at ASPET Journals on March 20, 2024

JPET Fast Forward. Published on April 7, 2017 as DOI: 10.1124/jpet.116.239707
This article has not been copyedited and formatted. The final version may differ from this version.

OHNO, A., SAITO, Y., HANIOKA, N., JINNO, H., SAEKI, M., ANDO, M., OZAWA, S. & SAWADA, J. 2004. Involvement of human hepatic UGT1A1, UGT2B4, and UGT2B7 in the glucuronidation of carvedilol. *Drug Metab Dispos,* 32**,** 235-9.

OHNO, S. & NAKAJIN, S. 2009. Determination of mRNA expression of human UDP-glucuronosyltransferases and application for localization in various human tissues by real-time reverse transcriptase-polymerase chain reaction. *Drug Metab Dispos,* 37**,** 32-40.

PASQUINELLI, A. E. 2012. MicroRNAs and their targets: recognition, regulation and an emerging reciprocal relationship. *Nat Rev Genet,* 13**,** 271-82.

RAUNGRUT, P., UCHAIPICHAT, V., ELLIOT, D. J., JANCHAWEE, B., SOMOGYI, A. A. & MINERS, J. O. 2010. In vitro-in vivo extrapolation predicts drug-drug interactions arising from inhibition of codeine glucuronidation by dextropropoxyphene, fluconazole, ketoconazole, and methadone in humans. *J Pharmacol Exp Ther,* 334**,** 609-18.

RITTER, J. K., CHEN, F., SHEEN, Y. Y., LUBET, R. A. & OWENS, I. S. 1992. Two human liver cDNAs encode UDP-glucuronosyltransferases with 2 log differences in activity toward parallel substrates including hyodeoxycholic acid and certain estrogen derivatives. *Biochemistry,* 31**,** 3409-14.

SAETROM, P., HEALE, B. S., SNOVE, O., JR., AAGAARD, L., ALLUIN, J. & ROSSI, J. J. 2007. Distance constraints between microRNA target sites dictate efficacy and cooperativity. *Nucleic Acids Res,* 35**,** 2333-42.

SEO, K. A., BAE, S. K., CHOI, Y. K., CHOI, C. S., LIU, K. H. & SHIN, J. G. 2010. Metabolism of 1'- and 4-hydroxymidazolam by glucuronide conjugation is largely mediated by UDP-glucuronosyltransferases 1A4, 2B4, and 2B7. *Drug Metab Dispos,* 38**,** 2007-13.

TANG, W., JIANG, Y., MU, X., XU, L., CHENG, W. & WANG, X. 2014. MiR-135a functions as a tumor suppressor in epithelial ovarian cancer and regulates HOXA10 expression. *Cell Signal,* 26**,** 1420-6.

THEODORE, S. C., DAVIS, M., ZHAO, F., WANG, H., CHEN, D., RHIM, J., DEAN-COLOMB, W., TURNER, T., JI, W., ZENG, G., GRIZZLE, W. & YATES, C. 2014. MicroRNA profiling of novel African American and Caucasian Prostate Cancer cell lines reveals a reciprocal regulatory relationship of miR-152 and DNA methyltranferase 1. *Oncotarget,* 5**,** 3512-25.

TURGEON, D., CARRIER, J. S., LEVESQUE, E., HUM, D. W. & BELANGER, A. 2001. Relative enzymatic activity, protein stability, and tissue distribution of human steroid-metabolizing UGT2B subfamily members. *Endocrinology,* 142**,** 778-787.

UCHAIPICHAT, V., MACKENZIE, P. I., GUO, X. H., GARDNER-STEPHEN, D., GALETIN, A., HOUSTON, J. B. & MINERS, J. O. 2004. Human udp-glucuronosyltransferases: isoform selectivity and kinetics of 4-methylumbelliferone and 1-naphthol glucuronidation, effects of organic solvents, and inhibition by diclofenac and probenecid. *Drug Metab Dispos,* 32**,** 413-23.

UCHAIPICHAT, V., SUTHISISANG, C. & MINERS, J. O. 2013. The glucuronidation of R- and S-lorazepam: human liver microsomal kinetics, UDP-glucuronosyltransferase enzyme selectivity, and inhibition by drugs. *Drug Metab Dispos,* 41**,** 1273-84.

WANG, Y., FU, J., JIANG, M., ZHANG, X., CHENG, L., XU, X., FAN, Z., ZHANG, J., YE, Q. & SONG, H. 2014. MiR-410 is overexpressed in liver and colorectal tumors and enhances tumor cell growth by silencing FHL1 via a direct/indirect mechanism. *PLoS One,* 9**,** e108708.

Downloaded from jpet.aspetjournals.org at ASPET Journals on March 20, 2024

JPET Fast Forward. Published on April 7, 2017 as DOI: 10.1124/jpet.116.239707
This article has not been copyedited and formatted. The final version may differ from this version.

WIJAYAKUMARA, D. D., HU, D. G., MEECH, R., MCKINNON, R. A. & MACKENZIE, P. I. 2015. Regulation of Human UGT2B15 and UGT2B17 by miR-376c in Prostate Cancer Cell Lines. *J Pharmacol Exp Ther,* 354**,** 417-25.

WILLIAMS, J. A., HYLAND, R., JONES, B. C., SMITH, D. A., HURST, S., GOOSEN, T. C., PETERKIN, V., KOUP, J. R. & BALL, S. E. 2004. DRUG-DRUG INTERACTIONS FOR UDP-GLUCURONOSYLTRANSFERASE SUBSTRATES: A PHARMACOKINETIC EXPLANATION FOR TYPICALLY OBSERVED LOW EXPOSURE (AUCI/AUC) RATIOS. *Drug Metabolism and Disposition,* 32**,** 1201-1208.

ZENG, Y. B., LIANG, X. H., ZHANG, G. X., JIANG, N., ZHANG, T., HUANG, J. Y., ZHANG, L. & ZENG, X. C. 2016. miRNA-135a promotes hepatocellular carcinoma cell migration and invasion by targeting forkhead box O1. *Cancer Cell Int,* 16**,** 63.

Downloaded from jpet.aspetjournals.org at ASPET Journals on March 20, 2024

JPET Fast Forward. Published on April 7, 2017 as DOI: 10.1124/jpet.116.239707
This article has not been copyedited and formatted. The final version may differ from this version.

Footnotes

This work was supported by funding from the National Health and Medical Research Council of Australia: [ID1020931] to P. I. Mackenzie; [ID1085410] to R. Meech, P. I. Mackenzie, R. A. McKinnon. The project was also supported by funding from the Flinders Medical Centre Foundation, Adelaide Australia. R.A.M. is a Cancer Council/SA Health Beat Cancer Professorial Chair. During the preparation period P.I.M. was a NHMRC Senior Principal Research Fellow; R.M. was an Australian Research Council Future Fellow.

Downloaded from jpet.aspetjournals.org at ASPET Journals on March 20, 2024

JPET Fast Forward. Published on April 7, 2017 as DOI: 10.1124/jpet.116.239707
This article has not been copyedited and formatted. The final version may differ from this version.

Legends

Figure 1. Effects of miRNA mimics on a luciferase reporter containing the UGT2B7 3'UTR or UGT2B4 3'UTR and expression of miRNAs in HepG2 cells. HepG2 cells were co-transfected with 30 nM miR-neg or miRNA mimics targeting individual miRNAs, Renilla reporter vector as control, and a luciferase reporter containing UGT2B7 3'UTR (A) or UGT2B4 3'UTR (B). Luciferase activity assays were performed as described in Methods; the luciferase activity of the reporter co-transfected with miRNA mimics is presented relative to that of the reporter cotransfected with miR-neg (set as a value of 100%). Data shown are mean ± S.E.M from four (in A) or two (in B) independent experiments performed in quadruplicates ***$p<0.0005$, **$p<0.005$. (C) The expression levels of miRNAs in HepG2 cells were measured using RT-qPCR, normalised toRNU6-2, and then presented relative to that of miR-410-3p (set at a value of 1). Data shown are mean ± S.E.M from a single experiment in triplicate.

Figure 2. A functional miR-3664-3p target site in the UGT2B7 3' UTR. (A) Shown are the position of a miR-3664-3p target site in the UGT2B7 3'-UTR and the sequence complementarity between this site and miR-3664-3p, including seed pairing (highlighted in grey) and substantial 3'-sequence pairing. The nucleotides of the miR-3664-3p sites are numbered relative to the stop codon (TAG with G positioned as -1) (NM_001074.3). (B) The mutation of CCTC to AGCT (boxed) that abolished the seed pairing between the miR-3664-3p target site and miR-3664-3p is shown. (C and D) Cotransfection of UGT2B7 3'-UTR luciferase reporter carrying either the wild-type or mutated miR-3664-3p site, 30 nM miR-neg or miR-3664-3p mimics, and Renilla reporter vector as control in HepG2 (C) and HuH7 (D), and 24 hours post-transfection, cells were harvested for luciferase activity assays as

Downloaded from jpet.aspetjournals.org at ASPET Journals on March 20, 2024

JPET Fast Forward. Published on April 7, 2017 as DOI: 10.1124/jpet.116.239707
This article has not been copyedited and formatted. The final version may differ from this version.

described in Methods. The luciferase activity of the reporter cotransfected with miR-3664-3p is presented relative to that of the reporter cotransfected with miR-neg (set as a value of 100%). Data shown are mean ± S.E.M from three (in C) or two (D) independent experiments performed in quadruplicates ***p<0.0005, **p<0.005.

Figure 3. miR-3664-3p mimics reduce the expression and activity of endogenous UGT2B7, and miR-3664 levels are negatively correlated to UGT2B7 mRNA in a tissue RNA panel. HepG2 cells were transfected with miR-3664-3p mimics (or miR-3664-3p inhibitor) or miR-neg. Cells were harvested for (1) analysis of UGT2B7 mRNA levels by RT-qPCR (A), (2) analysis of UGT2B7 protein levels by western blotting (C), and (3) analysis of UGT2B7 activity via morphine glucuronidation assays (D) as described in Methods. (A and B) UGT2B7 and GAPDH mRNA levels in cells transfected with miR-3664-3p mimics (or miR-3664-3p inhibitors) are presented relative to that in cells transfected the negative control miR-neg. Data shown are mean ± S.E.M. from three independent experiments performed in triplicates, ***p<0.0005. (C) UGT2B7 and calnexin protein immunosignals from a representative western blot experiment (top); quantification of UGT2B7 protein levels (means ± S.E.M. from two independent experiments performed in triplicate) in cells transfected miR-3664-3p mimics relative to cells transfected with miR-neg (bottom). *P < 0.05. (D) Morphine-glucuronidation activity in miR-3664-3p mimic-transfected cells relative to that of miR-neg-transfected cells (set as a value of 100%). Data shown are means ± S.E.M. from two independent experiments performed in triplicate. **P < 0.005. (E) miR-3664 and UGT2B4 mRNA levels in a panel of 10 normal tissues were measured using RT-qPCR as described in Methods. Shown is a Spearman's correlation analysis between the expression levels of miR-3664-3p and UGT2B4 mRNA in this human tissue panel.

Downloaded from jpet.aspetjournals.org at ASPET Journals on March 20, 2024

JPET Fast Forward. Published on April 7, 2017 as DOI: 10.1124/jpet.116.239707
This article has not been copyedited and formatted. The final version may differ from this version.

Figure 4.

A functional miR-135a-5p site and a functional miR-410-3p in the UGT2B4 3' UTR. (A) Shown are the positions of the miR-135a-5p and the miR-410-3p target site in the UGT2B4 3'-UTR and the sequence complementarity between these two sites and their cognate miRNAs, including seed pairing (highlighted in grey) and 3'-sequence pairing. The nucleotides of the two miRNA sites are numbered relative to the stop codon (TAG with G positioned as -1) (NM_021139.2). (B) The mutation of GCCA to TGAC (boxed) that abolishes the seed pairing between the miR-135a-5p target site and miR-135a-5p and the mutation of TATA to CCGC (boxed) that abolishes the seed pairing between the miR-410-3p target site and miR-410-3p is shown. (C and D) Cotransfection of a UGT2B4 3'-UTR luciferase reporter carrying either a wild-type or mutated miR-135a-5p target site, 30 nM miR-neg or miR-135a-5p mimics, and Renilla reporter vector as control in HepG2 (C) and HuH7 cells (D). (E) Cotransfection of a UGT2B4 3'-UTR luciferase reporter carrying either a wild-type or mutated miR-410-3p target site, 30 nM miR-neg or miR-410-3p mimics, and Renilla reporter vector as control in HepG2 cells. 24 hours post-transfection, cells were harvested for luciferase activity assays as described in Methods. The luciferase activity of the reporter cotransfected with miRNA mimics is presented relative to that of the reporter cotransfected with miR-neg (set as a value of 100%). Data shown are mean ± S.E.M from two independent experiments performed in quadruplicates *<0.05, **p<0.005, ***p<0.0005.

Figure 5. miR-135a-5p and miR-410-3p mimics reduce UGT2B4 mRNA levels in HuH7 cells, and correlation analyses between UGT2B4 and miR-135a-5p (or miR-410-3p) levels in human tissue panels and liver cancer specimens. (A and B) HuH7 cells were transfected with

Downloaded from jpet.aspetjournals.org at ASPET Journals on March 20, 2024

JPET Fast Forward. Published on April 7, 2017 as DOI: 10.1124/jpet.116.239707
This article has not been copyedited and formatted. The final version may differ from this version.

either miR-neg, miR-135a-5p, or miR-410-3p) mimics. UGT2B4 and GAPDH mRNA levels were measured using RT-qPCR. The UGT2B4 mRNA levels in miRNA mimic-transfected cells are presented relative to that of cells transfected miR-neg (set at a value of 100%). Data shown are mean ±S.E.M. from two independent experiments performed in triplicates. *$p<0.05$, **$p<0.005$. (C and E) The expression levels of UGT2B4 mRNA, miR-135a-5p, and miR-410-3p in a human tissue panel (C) and a panel of normal human liver tissues (E) were quantified using RT-qPCR followed by correlation analyses between miR-135a-5p (or miR-410-3p) and UGT2B4 mRNA levels using GraphPad Prism 6 software as described in Methods. (D) Transcriptome profiling data (RNAseq and miRNAseq) from a cohort of Liver Hepatocellular Carcinomas (LIHC) were downloaded from the Cancer Genome Atlas (TCGA) data portal. Data was normalized and a correlation analysis between miR-410 and UGT2B4 mRNA levels was conducted using Spearman's rank method; the graph was drawn using statistical package R as described in Methods.

Downloaded from jpet.aspetjournals.org at ASPET Journals on March 20, 2024

JPET Fast Forward. Published on April 7, 2017 as DOI: 10.1124/jpet.116.239707
This article has not been copyedited and formatted. The final version may differ from this version.

Table 1. Primers used for cloning, site-directed mutagenesis and RT-qPCR

Primer	Sequence (5' - 3')
Cloning	
UGT2B7_3'UTR_F	CCGCTCTAGATTATATCTGAGATTTGAAGC
UGT2B7_3'UTR_R	CCGGTCTAGACCGTAGTGTTTTCTTCATTG
UGT2B4_3'UTR_F	CCGGTCTAGATTACGTCTGAGGCTGGAAGC
UGT2B4_3'UTR_R	CCGATCTAGAGCTTCCTCAACAACAGTTAA
Site-directed mutagenesis	
2B7_miR3664_MT_F	AGATTTCTTTCTTAGCTAGACAAAAAAAAAAAAG
2B7_miR3664_MT_R	TTTTTTTTTTTTGTCTAGCTAAGAAAGAAATCTTG
2B4_miR135a_MT_F	CAAAAATGATATAAATGACTATGAGGTTATATTG
2B4_miR135a_MT_R	CAATATAACCTCATAGTCATTTATATCATTTTTG
2B4_miR410_MT_F	AAAGCCATATGAGGTCCGCTTGAAATGTATTGAG
2B4_miR410_MT_R	CTCAATACATTTCAAGCGGACCTCATATGGCTTT
RT-qPCR	
miR3664-3p_qPCR_F	GCAGTCTCAGGAGTAAAGACA
miR3664-3p_qPCR_R	AGGTCCAGTTTTTTTTTTTTTTTAACTC
miR-1266-5p_qPCR_F	GCC TCA GGG CTG TAG AAC A
miR-1266-5p_qPCR_R	GTC CAG TTT TTT TTT TTT TTT AGC CC
miR-4483_qPCR_F	GCA GGG GGT GGT CTG T
miR-4483_qPCR_R	GGT CCA GTT TTT TTT TTT TTT TCA ACA
miR-4317_qPCR_F	GCA GAC ATT GCC AGG GA
miR-4317_qPCR_R	CAG GTC CAG TTT TTT TTT TTT TTT AAA C
miR-216b-5p_qPCR_F	GCA GAA ATC TCT GCA GGC A
miR-216b-5p_qPCR_R	GGT CCA GTT TTT TTT TTT TTT TTC ACA TT
miR-135a_qPCR_F	CGC AGT ATG GCT TTT TAT TCC T
miR-135a_qPCR_R	GGT CCA GTT TTT TTT TTT TTT TTC ACA T
miR-410_qPCR_F	CGC AGA ATA TAA CAC AGA TGG C
miR-410_qPCR_R	AGG TCC AGT TTT TTT TTT TTT TTA CAG
miR-489_qPCR_F	CGC AGG TGA CAT CAC ATA TAC
miR-489_qPCR_R	CCA GTT TTT TTT TTT TTT TGC TGC C
miR-4691-5p_qPCR_F	GGT CCT CCA GGC CAT GA
miR-4691-5p_qPCR_R	AGT TTT TTT TTT TTT TTC CGC AGC
miR-101_qPCR_F	CGC AGT ACA GTA CTG TGA TA
miR-101_qPCR_R	GGT CCA GTT TTT TTT TTT TTT TTT CAG T

Downloaded from jpet.aspetjournals.org at ASPET Journals on March 20, 2024

Figure 1

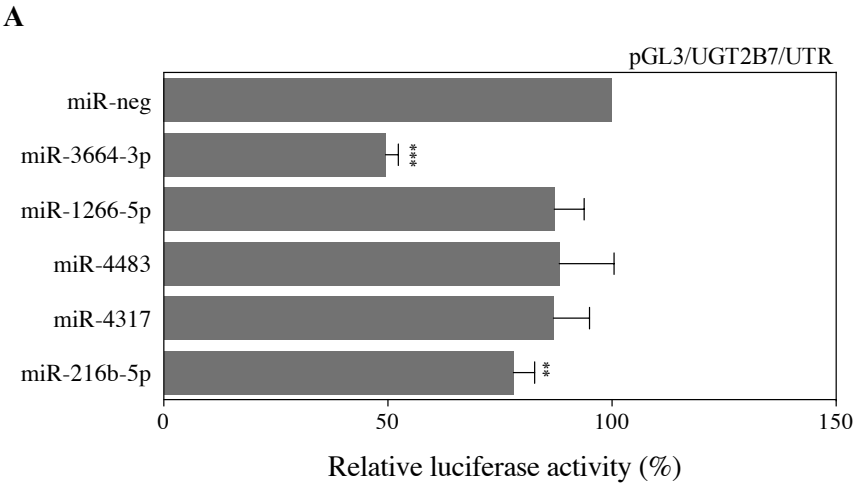
A
pGL3/UGT2B7/UTR
miR-neg
miR-3664-3p
miR-1266-5p
miR-4483
miR-4317
miR-216b-5p
***
**
0
50
100
150
Relative luciferase activity (%)

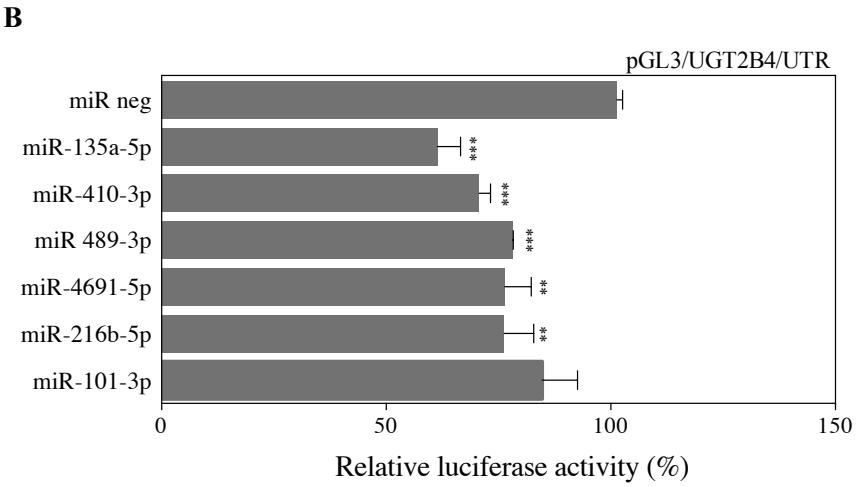
B
pGL3/UGT2B4/UTR
miR neg
miR-135a-5p
miR-410-3p
miR 489-3p
miR-4691-5p
miR-216b-5p
miR-101-3p
***
***
***
**
**
0
50
100
150
Relative luciferase activity (%)

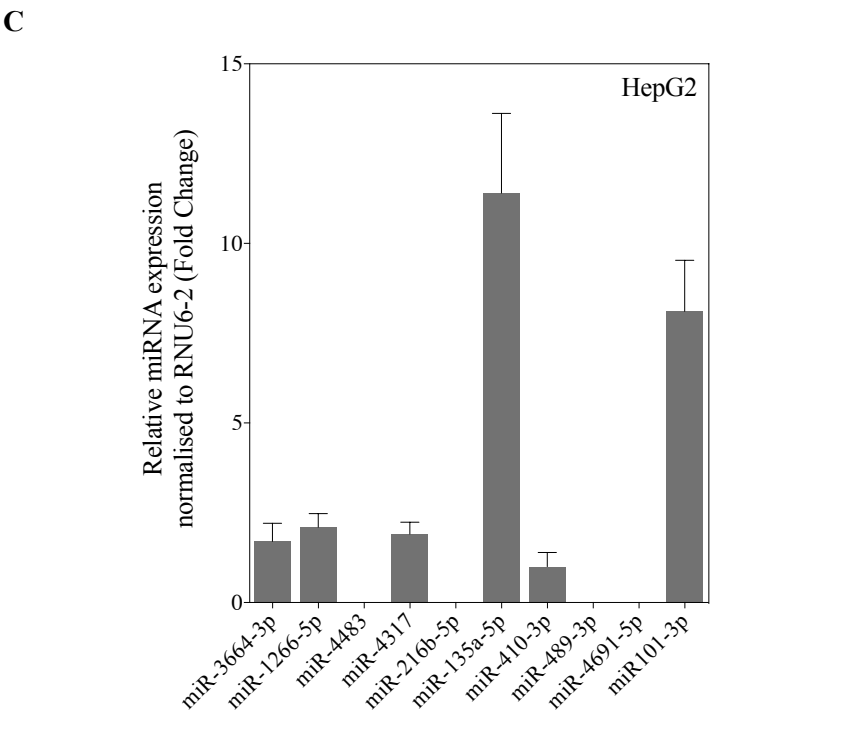
C
HepG2
Relative miRNA expression
normalised to RNU6-2 (Fold Change)
15
10
5
0
miR-3664-3p
miR-1266-5p
miR-4483
miR-4317
miR-216b-5p
miR-135a-5p
miR-410-3p
miR-489-3p
miR-4691-5p
miR101-3p

Figure 2

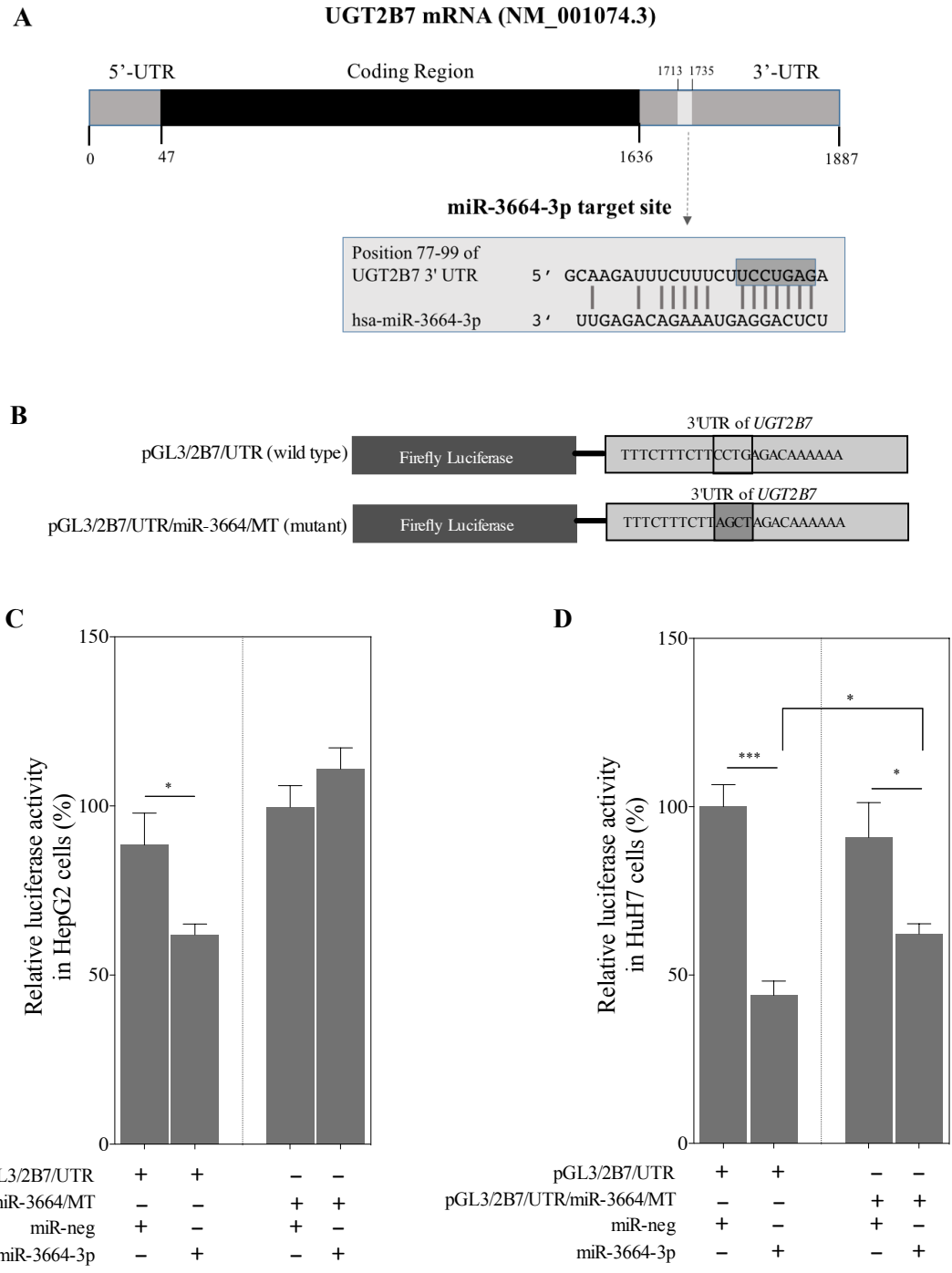
A
UGT2B7 mRNA (NM_001074.3)
5'-UTR
Coding Region
1713 1735
3'-UTR
0
47
1636
1887
miR-3664-3p target site
Position 77-99 of
UGT2B7 3' UTR
5′ GCAAGAUUUCUUUCUUCCUGAGA
hsa-miR-3664-3p
3′ UUGAGACAGAAAUGAGGACUCU
B
3'UTR of UGT2B7
pGL3/2B7/UTR (wild type)
Firefly Luciferase
TTTCTTTCTTCCTGAGACAAAAAA
3'UTR of UGT2B7
pGL3/2B7/UTR/miR-3664/MT (mutant)
Firefly Luciferase
TTTCTTTCTTAGCTAGACAAAAAA
C
Relative luciferase activity in HepG2 cells (%)
150
100
50
0
*
pGL3/2B7/UTR + + – –
pGL3/2B7/UTR/miR-3664/MT – – + +
miR-neg + – + –
miR-3664-3p – + – +
D
Relative luciferase activity in HuH7 cells (%)
150
100
50
0
***
*
*
pGL3/2B7/UTR + + – –
pGL3/2B7/UTR/miR-3664/MT – – + +
miR-neg + – + –
miR-3664-3p – + – +

Figure 3

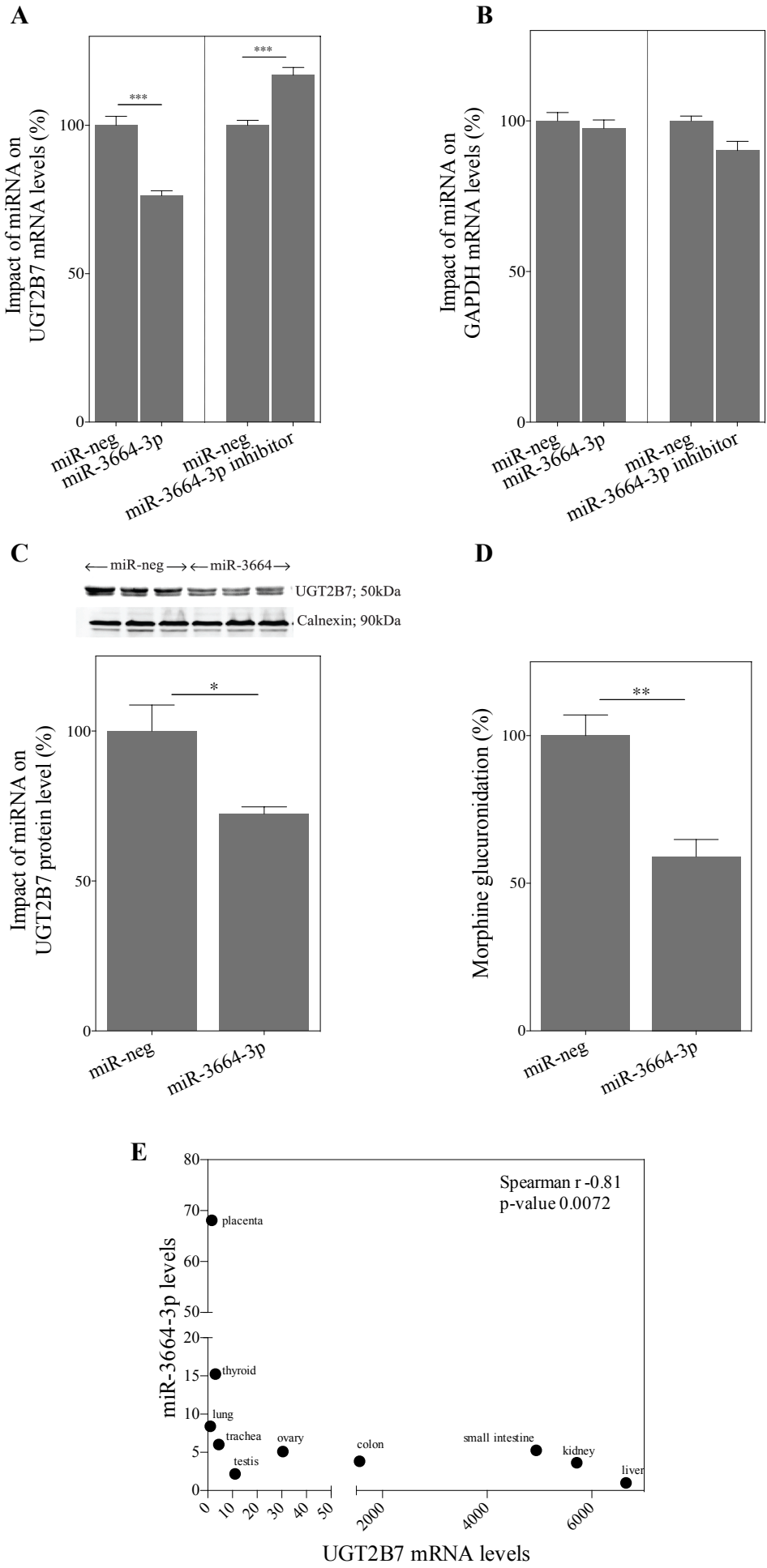
A
Impact of miRNA on UGT2B7 mRNA levels (%)
***
***
100
50
0
miR-neg
miR-3664-3p
miR-neg
miR-3664-3p inhibitor
B
Impact of miRNA on GAPDH mRNA levels (%)
100
50
0
miR-neg
miR-3664-3p
miR-neg
miR-3664-3p inhibitor
C
← miR-neg → ← miR-3664 →
UGT2B7; 50kDa
Calnexin; 90kDa
Impact of miRNA on UGT2B7 protein level (%)
*
100
50
0
miR-neg
miR-3664-3p
D
Morphine glucuronidation (%)
**
100
50
0
miR-neg
miR-3664-3p
E
Spearman r -0.81
p-value 0.0072
miR-3664-3p levels
placenta
thyroid
lung
trachea
ovary
testis
colon
small intestine
kidney
liver
UGT2B7 mRNA levels

Figure 4

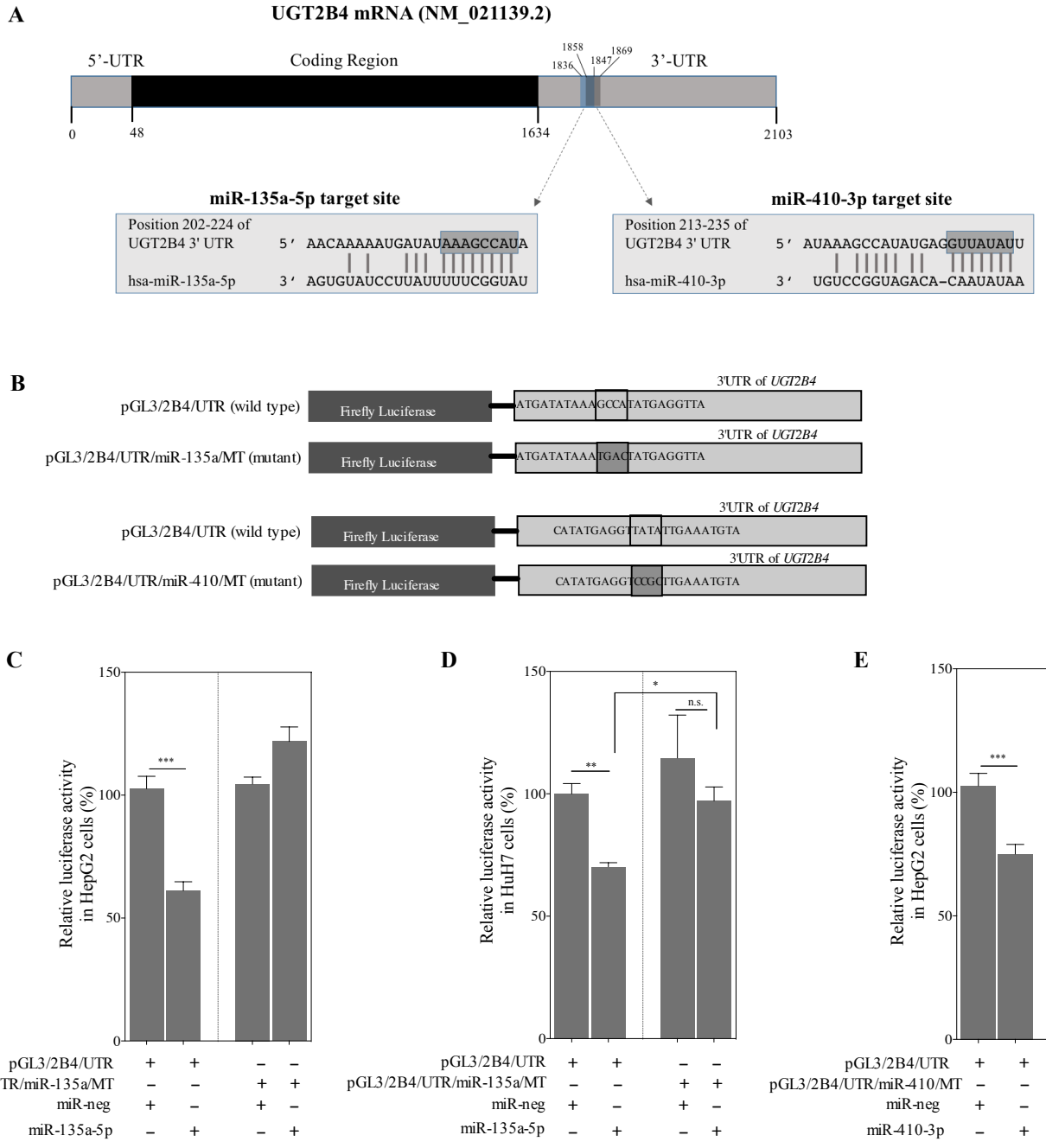
A
UGT2B4 mRNA (NM_021139.2)
5'-UTR
Coding Region
3'-UTR
1858
1836
1847
1869
0
48
1634
2103
miR-135a-5p target site
Position 202-224 of UGT2B4 3' UTR
5' AACAAAAAUGAUAUAAAGCCAUA
hsa-miR-135a-5p
3' AGUGUAUCCUUAUUUUUCGGUAU
miR-410-3p target site
Position 213-235 of UGT2B4 3' UTR
5' AUAAAGCCAUAUGAGGUUAUAUU
hsa-miR-410-3p
3' UGUCCGGUAGACA-CAAUAUAA
B
pGL3/2B4/UTR (wild type)
Firefly Luciferase
3'UTR of UGT2B4
ATGATATAAAGCCATATGAGGTTA
pGL3/2B4/UTR/miR-135a/MT (mutant)
ATGATATAAATGACTATGAGGTTA
pGL3/2B4/UTR (wild type)
CATATGAGGTTATATTGAAATGTA
pGL3/2B4/UTR/miR-410/MT (mutant)
CATATGAGGTCCGCTTGAAATGTA
C
Relative luciferase activity in HepG2 cells (%)
150
100
50
0
***
pGL3/2B4/UTR + + – –
pGL3/2B4/UTR/miR-135a/MT – – + +
miR-neg + – + –
miR-135a-5p – + – +
D
Relative luciferase activity in HuH7 cells (%)
**
*
n.s.
pGL3/2B4/UTR + + – –
pGL3/2B4/UTR/miR-135a/MT – – + +
miR-neg + – + –
miR-135a-5p – + – +
E
Relative luciferase activity in HepG2 cells (%)
***
pGL3/2B4/UTR + + – –
pGL3/2B4/UTR/miR-410/MT – – + +
miR-neg + – + –
miR-410-3p – + – +

Figure 5

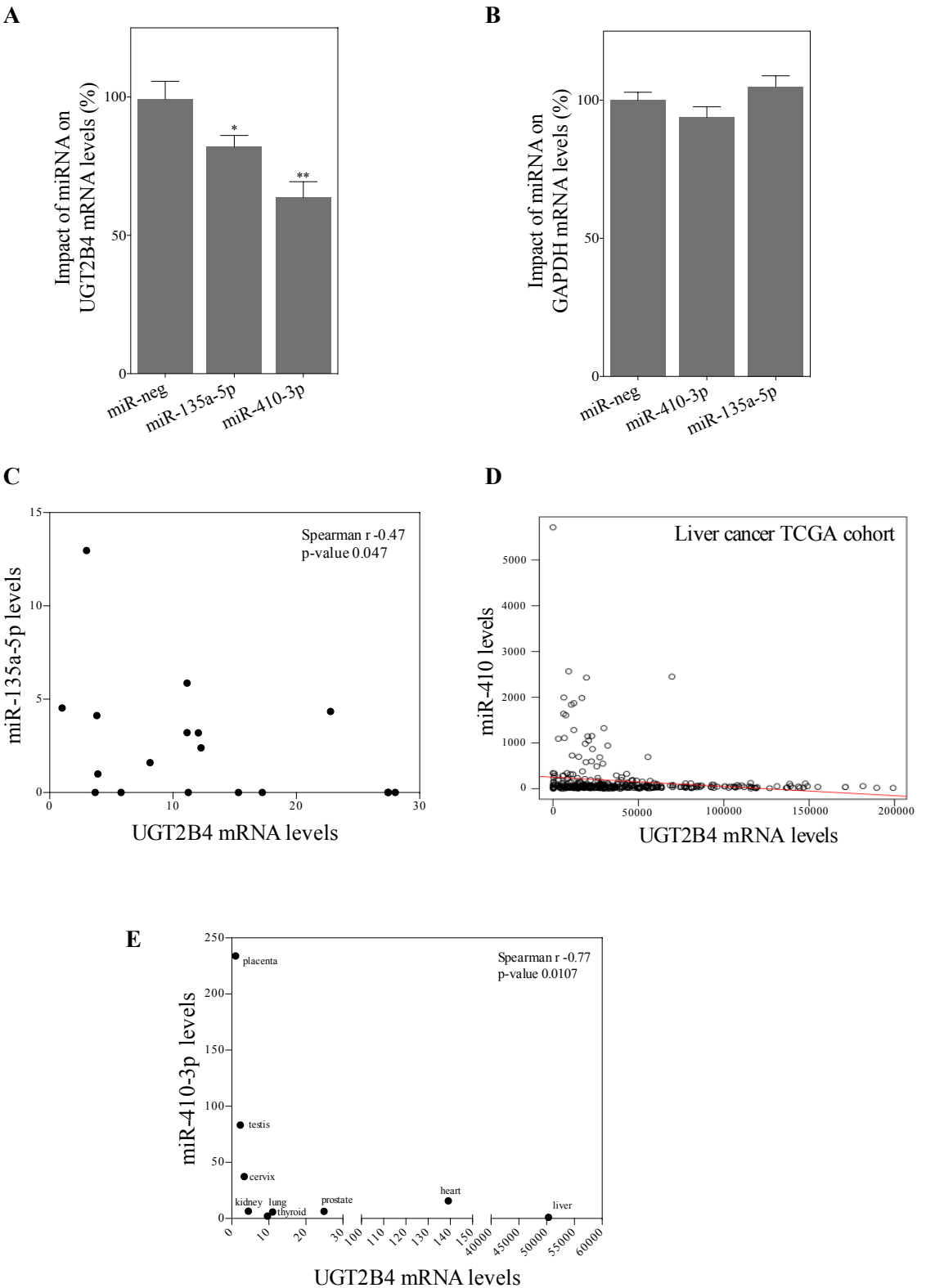
A
Impact of miRNA on UGT2B4 mRNA levels (%)
100
50
0
*
**
miR-neg
miR-135a-5p
miR-410-3p
B
Impact of miRNA on GAPDH mRNA levels (%)
100
50
0
miR-neg
miR-410-3p
miR-135a-5p
C
Spearman r -0.47
p-value 0.047
miR-135a-5p levels
15
10
5
0
0
10
20
30
UGT2B4 mRNA levels
D
Liver cancer TCGA cohort
miR-410 levels
5000
4000
3000
2000
1000
0
0
50000
100000
150000
200000
UGT2B4 mRNA levels
E
Spearman r -0.77
p-value 0.0107
miR-410-3p levels
250
200
150
100
50
0
placenta
testis
cervix
kidney
lung
thyroid
prostate
heart
liver
0
10
20
30
100
110
120
130
140
150
40000
45000
50000
55000
60000
UGT2B4 mRNA levels

Journal of Pharmacology and Experimental Therapeutics (JPET)

Supplemental material for 'Regulation of UGT2B4 and UGT2B7 by miRNAs in liver cancer cells'

Dhilushi D Wijayakumara, Peter I Mackenzie, Ross A McKinnon, Dong Gui Hu* and Robyn Meech*

Supplemental Figure Legends:

Supplemental Figure 1. Schematic of the UGT2B4 and UGT2B7 3'-UTR regions with predicted miRNA binding sites indicated by boxes.

Supplemental Figure 2. UGT2B4 and miR-135a-5p levels were measured in HepG2 and HuH7 cells. The expression of UGT2B4 in HepG2 cells is set as 1 (after normalising to 18S RNA) showing that UGT2B4 has higher expression in HepG2 than HuH7 cells. The expression of miR-135a-5p in HuH7 cells is set as 1 (after normalising to RNU6-2) showing that miR-135a-5p has higher expression in HepG2 than in HuH7 cells. Data are means from an experiment performed in quadruplicate, the error bar represents 1S.D., **$p<0.005$, ***$p<0.0005$.

Supplemental Figure 3. Correlation analysis of UGT2B4 and miR-135a primary transcript levels in the TCGA liver cancer cohort (370 specimens). Both the miR-135a-1 and miR135a-2 genes were examined because they both give rise to mature miR-135a-5p. No significant correlation was observed between UGT2B4 and either miR-135a-1 or miR-135a-2 (UGT2B4/miR-135a-1 rho value = 0.040, p value = 0.43959; UGT2B4/miR-135a-2 rho value = 0.0055, p value = 0.9152).

Supplementary Figure 1

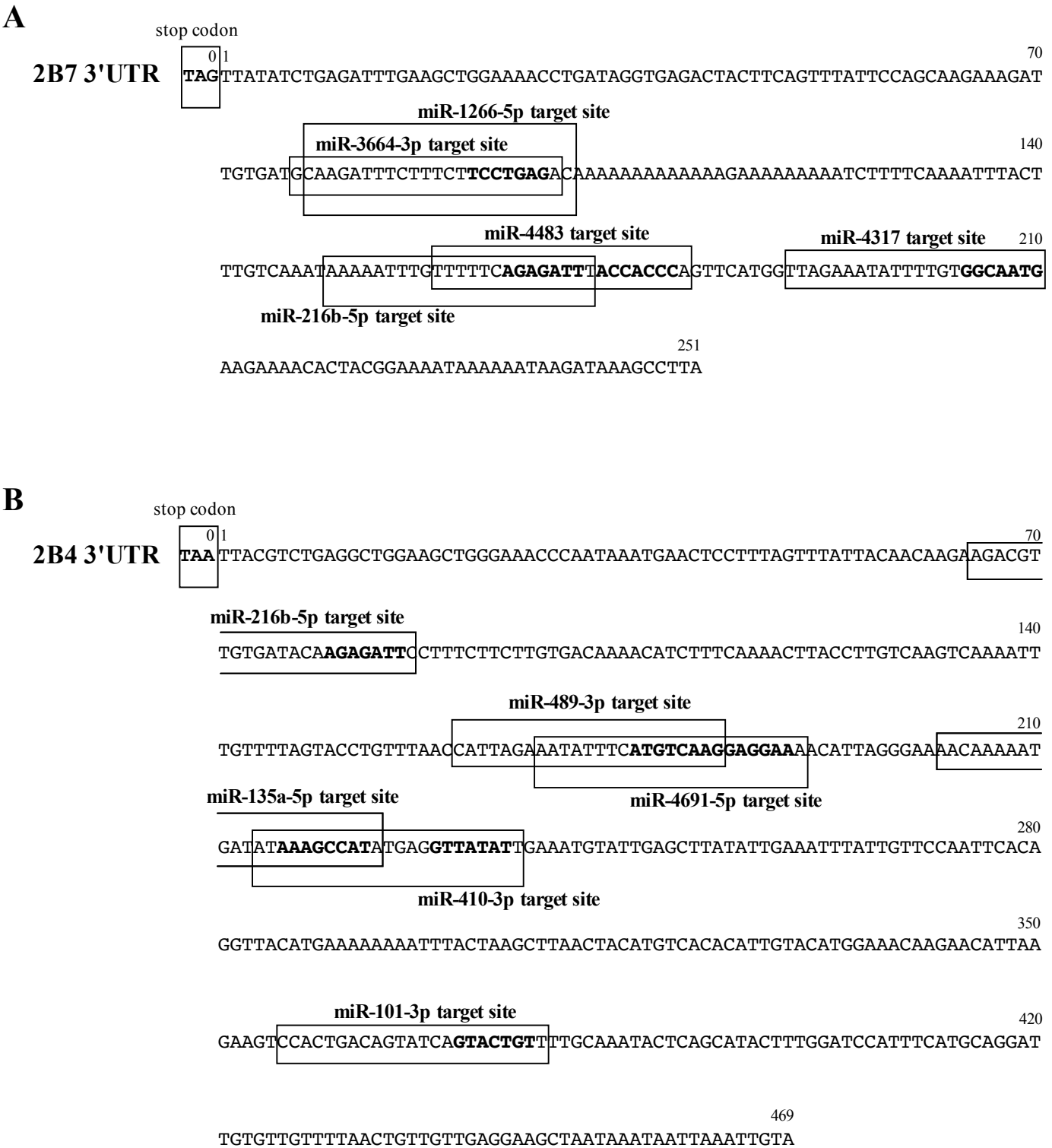

Supplementary Figure 2

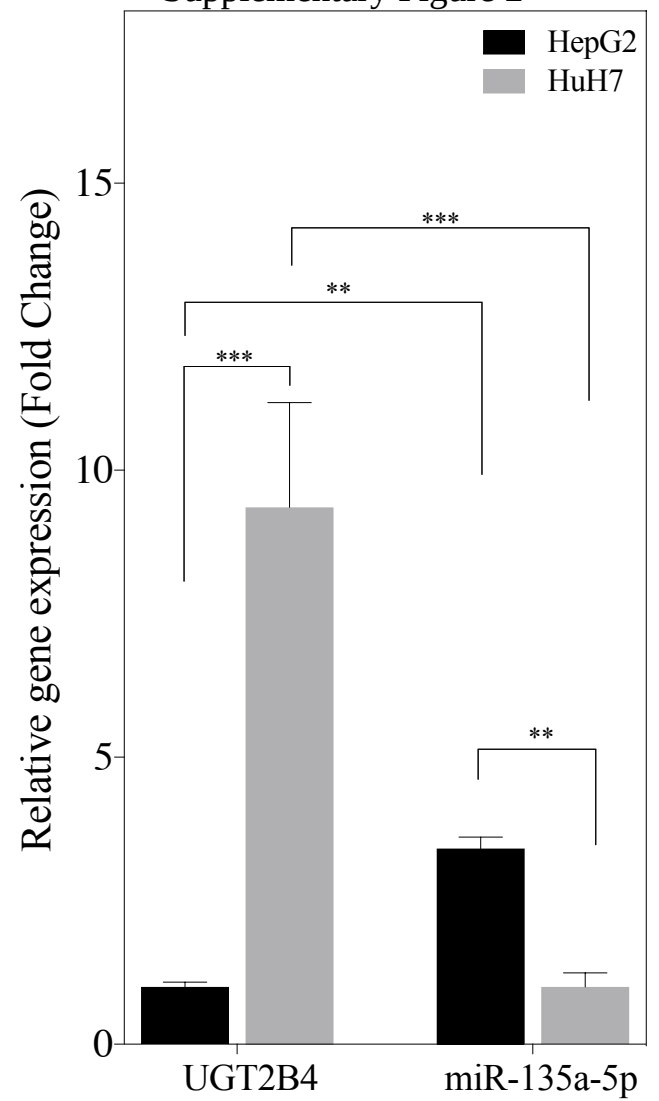
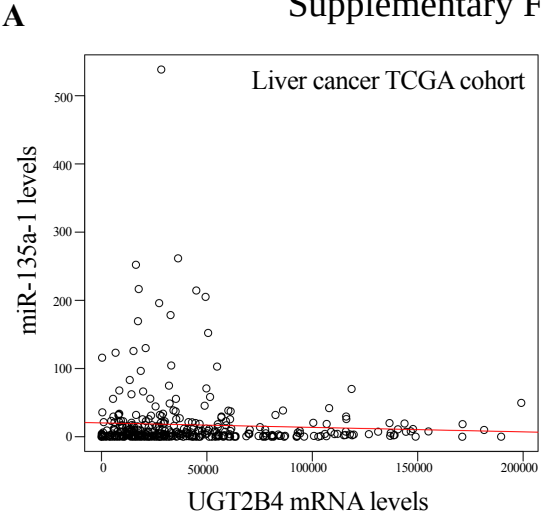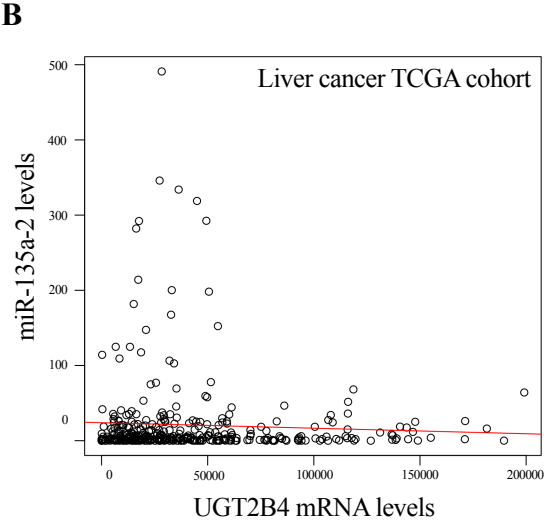
Supplementary Figure 3